

Critical Scaling and Continuum Limits in the $D > 1$ Kazakov–Migdal Model

Yu. Makeenko¹

*Institute of Theoretical and Experimental Physics,
B. Cheremushkinskaya 25, 117259 Moscow, Russian Federation*

and

*The Niels Bohr Institute,
Blegdamsvej 17, 2100 Copenhagen, Denmark*

Abstract

I investigate the Kazakov–Migdal (KM) model — the Hermitean gauge-invariant matrix model on a D -dimensional lattice. I utilize an exact large- N solution of the KM model with a logarithmic potential to examine its critical behavior. I find critical lines associated with $\gamma_{str} = -1/2$ and $\gamma_{str} = 0$ as well as a tri-critical point associated with a Kosterlitz–Thouless phase transition. The continuum theories are constructed expanding around the critical points. The one associated with $\gamma_{str} = 0$ coincides with the standard $d = 1$ string while the Kosterlitz–Thouless phase transition separates it from that with $\gamma_{str} = -1/2$ which is indistinguishable from pure $2D$ gravity for local observables but has a continuum limit for correlators of extended Wilson loops at large distances due to a singular behavior of the Itzykson–Zuber correlator of the gauge fields. I reexamine the KM model with an arbitrary potential in the large- D limit and show that it reduces at large N to a one-matrix model whose potential is determined self-consistently. A relation with discretized random surfaces is established via the gauged Potts model which is equivalent to the KM model at large N providing the coordination numbers coincide.

¹E-mail: makeenko@vxitep.itep.msk.su / makeenko@nbivax.nbi.dk

1 Introduction

Matrix models are usually associated with discretized random surfaces or strings in a $d \leq 1$ -dimensional embedding space and, in particular, with two-dimensional quantum gravity. The simplest Hermitean one-matrix model corresponds to pure gravity while a chain of Hermitean matrices describes two-dimensional gravity interacting with $d \leq 1$ matter. The long-standing problem with this approach is that the stringy phase does not exist above the $d=1$ barrier (see Ref. [1] for a review).

A natural multi-dimensional extension of this construction is the Kazakov–Migdal (KM) model [2] which is defined by the partition function

$$Z_{KM} = \int \prod_{\{x,y\}} dU_{xy} \prod_x d\phi_x e^{N \text{tr} \left(-\sum_x V(\phi_x) + c \sum_{\{x,y\}} \phi_x U_{xy} \phi_y U_{xy}^\dagger \right)}. \quad (1.1)$$

Here the integration over the gauge field U_{xy} is over the Haar measure on $SU(N)$ at each link of a D -dimensional hypercubic lattice with x labeling its sites and $\{x,y\}$ labeling the link from the site x to the neighbor site y . The model (1.1) obviously recovers the standard open matrix chain if the lattice is just a one-dimensional sequence of points for which the gauge field can be absorbed by a unitary transformation of ϕ_x .

The KM model was originally introduced in the context of induced lattice gauge theories [2]. Its remarkable property is an existence of self-consistent scaling solutions with nontrivial critical indices [3] for a quartic potential V in (1.1) at large N and any D . Some other investigations of a critical behavior of the KM model have been performed recently [4, 5]. There is however a number of problems with the scaling solutions. In particular, it is not clear what physical system are they associated with.

From this point of view it is instructive to look at exact large- N solutions of the KM model and to pass to the continuum by approaching critical points. The only exact solutions of the KM model are known for quadratic [6] and logarithmic [7] potentials. The spectral density describing the distribution of eigenvalues of a x -independent saddle-point matrix, which dominates the path integral (1.1) at large N , is quite similar in both cases to that for a one-matrix model and was obtained by standard methods (see Ref. [8] for a review). The solution of the KM model with the logarithmic potential reduced [7] to algebraic equations for the end points of the eigenvalue support — the boundary equations.

In the present paper I investigate the boundary equations of the KM model with the logarithmic potential which explicitly determine the solution² and calculate specific heat (or string susceptibility) at large N . The model has a rich critical behavior: a critical line associated with $\gamma_{str} = -1/2$, a critical line associated with $\gamma_{str} = 0$ and a tri-critical point where a Kosterlitz–Thouless phase transition between these two phases occurs. In order to construct the continuum theories I perform an expansion around the critical points which is quite similar to the one for two-dimensional gravity. The continuum limit

²A similar analysis is performed in Ref. [9].

associated with $\gamma_{str} = 0$ coincides with the standard $d = 1$ string (or $2D$ gravity plus critical matter). A Kosterlitz–Thouless phase transition separates this phase from the one with $\gamma_{str} = -1/2$ which is indistinguishable from pure $2D$ gravity (or a $d = 0$ string) for local observables which live at the same site of the lattice. There is, however, another type of observables — extended Wilson loops — for which the continuum limit sets up at distances $L \sim 1/\sqrt{\varepsilon}$ (where ε characterizes deviation from the critical point) due to a singular behavior of the Itzykson–Zuber correlator of the gauge fields. This phenomenon occurs in the vicinity of the tri-critical point where the Itzykson–Zuber correlator changes its behavior.

In order to compare with previous results I reexamine the KM model in the large- D limit and show that at large N it reduces for arbitrary V in (1.1) and $c \sim 1/D$ to a one-matrix model whose potential is determined self-consistently. While this one-matrix model has generically $\gamma_{str} = -1/2$, one can obtain $\gamma_{str} = 1/(k+1)$ ($k \geq 1$) by tuning the value of c quite similarly to Refs. [10, 11, 12]. For the involved logarithmic potential one obtains in this way $\gamma_{str} = 0$ in agreement with exact solution.

In order to relate the KM model with discretized random surfaces and strings, I propose a matrix model — the gauged Potts model — which is equivalent to the KM model at large N providing the coordination numbers coincide. The gauged Potts model has a natural connection with discretized random surfaces and is convenient for interpreting the results obtained in this paper. The proof of equivalence of the gauged Potts and KM models is given via loop equations which reduce at large N to a one-link equation that is similar to the one for the Hermitean two-matrix model [13, 14, 15]. This reduction and, therefore, the equivalence hold in the strong coupling phase where the vacuum expectation values of the closed Wilson loops of the gauge field vanish except for those of vanishing minimal area.

This paper is organized as follows. Sect. 2 is devoted to the description of the KM model with the logarithmic potential, its one-cut solution at large N and the calculation of string susceptibility. Critical points and the phase structure of the model are obtained. In Sect. 3 an expansion around the critical points which specifies the continuum limits of the model is performed. The behavior of the Itzykson–Zuber correlator of gauge fields in the continuum is studied. In Sect. 4 the large- D limit of the KM model with an arbitrary potential is discussed. In Sect. 5 the gauged Potts model is introduced and its equivalence to the KM model at large N is proven. This section also contains a description of the large- N solution of these models. In Sect. 6 I discuss the results and some related problems for future investigations. Appendix A is devoted to a non-standard behavior of the eigenvalue support which leads to $\gamma_{str} = 0$. Appendix B contains a proof of the convolution formula for the continuum Itzykson–Zuber correlators which is used in Sect. 3. Appendix C contains the derivation of the loop equations which are considered in Sect. 5.

2 Explicit solution for logarithmic potential

The distribution of eigenvalues of ϕ_x for the KM model with the logarithmic potential coincides at large N with that for a one-matrix model which interpolates between cubic and Penner potentials and is solved in this section by the standard technique. The string susceptibility of the KM model with the logarithmic potential is calculated at large N . It reveals a rich critical behavior: a critical line associated with $\gamma_{str} = -1/2$, a critical line associated with $\gamma_{str} = 0$ and a tri-critical point where a Kosterlitz–Thouless phase transition occurs.

2.1 The KM model with logarithmic potential

Besides the Gaussian case [6] the only exact solution of the KM model (1.1) is known for the logarithmic potential [7]³

$$V(\phi_x) = -\alpha \log(b - \phi_x) - (2D - 1)(\alpha + 1) \log(a + \phi_x) + [(2D - 1)b - a]\phi_x. \quad (2.1)$$

We put for simplicity the coefficient in front of the kinetic term in (1.1) $c = 1$. The eigenvalue distribution of the (x -independent) saddle-point configuration coincides for the model (1.1) with the potential (2.1) and for the Hermitean one-matrix model with the potential

$$\tilde{V}(\phi) = -\alpha \log(b - \phi) + (\alpha + 1) \log(a + \phi) - (b + a)\phi, \quad (2.2)$$

which is recovered by the potential (2.1) at $D = 0$.

The potentials (2.1) and (2.2) can be simplified shifting ϕ_x by a constant value:

$$\phi_x = \hat{\phi}_x + \frac{b - a}{2} \mathbf{I}. \quad (2.3)$$

The corresponding shift of the kinetic term in the action is

$$\frac{\text{tr}}{N} \phi_x U_{xy} \phi_y U_{xy}^\dagger = \frac{\text{tr}}{N} \hat{\phi}_x U_{xy} \hat{\phi}_y U_{xy}^\dagger + \frac{b - a}{2} \left(\frac{\text{tr}}{N} \hat{\phi}_x + \frac{\text{tr}}{N} \hat{\phi}_y \right). \quad (2.4)$$

Absorbing the last term on the r.h.s. into the new potential, $\hat{V}(\hat{\phi})$, and introducing

$$\beta = \frac{a + b}{2}, \quad (2.5)$$

one gets

$$\hat{V}(\hat{\phi}_x) = -\alpha \log(\beta - \hat{\phi}_x) - (2D - 1)(\alpha + 1) \log(\beta + \hat{\phi}_x) + 2(D - 1)\beta \hat{\phi}_x \quad (2.6)$$

and

$$\hat{\hat{V}}(\hat{\phi}) = -\alpha \log(\beta - \hat{\phi}) + (\alpha + 1) \log(\beta + \hat{\phi}) - 2\beta \hat{\phi}. \quad (2.7)$$

³The parameter α is related to the original parameters of Ref. [7] as follows: $\alpha = ab + c$.

Note, that both Eqs. (2.6) and (2.7) can be straightforwardly obtained from Eqs. (2.1) and (2.2) substituting $a = b = \beta$.

The potential (2.6) depends on two parameters α and β . However, one more parameter η appears in the perturbative expansion when

$$\hat{\phi}_x = \eta \mathbf{I} + \phi_x \quad (2.8)$$

and the expansion goes in ϕ_x . Comparing with Eq. (2.3), one identifies η with $(a - b)/2$. Therefore, the expression (2.1) is convenient for the perturbative expansion.

The perturbative expansion starts from the Gaussian model which is characterized by the quadratic potential

$$V(\phi_x) = \frac{m_0^2}{2} \phi_x^2 \quad (2.9)$$

where

$$m_0^2 = \frac{a}{b} + (2D - 1) \frac{b}{a} \quad (2.10)$$

as it follows from (2.1) in the limit [7]

$$\alpha = ab, \quad a \sim b \rightarrow \infty \quad \text{and} \quad \phi_x \sim 1 \quad (\text{quadratic potential}). \quad (2.11)$$

The analogous parameter for the one-matrix model (2.2) is

$$\mu = \frac{a}{b} - \frac{b}{a}. \quad (2.12)$$

Solving the quadratic equation (2.10) for a/b versus m_0^2 and substituting into Eq. (2.12), one finds

$$\mu = \frac{(D - 1)m_0^2 + D\sqrt{m_0^4 - 4(2D - 1)}}{(2D - 1)} \quad (2.13)$$

which coincides with the solution of Ref. [6].

A more narrow region of the parameters than (2.11):

$$\alpha = ab, \quad a, b \rightarrow \infty, \quad (a - b) \sim \phi \sim b^{\frac{1}{3}}, \quad (2.14)$$

is of special interest because the potential (2.2) of the associated one-matrix model then reduces to a cubic one.

It is worth mentioning that the normalization of the parameters of the potential (2.1) is chosen to make (2.2) to be D independent. It were be more conventional to have instead a D -independent potential V moving the D -dependence to \tilde{V} . The Gaussian formulas (2.10) and (2.13) show how this can be done.

For purposes of the perturbative expansion it is useful to restore the hopping parameter c in front of the kinetic term, like it enters the exponent in Eq. (1.1). This can be achieved by the rescaling

$$\{\phi_x, b\} \rightarrow \sqrt{c}\{\phi_x, b\}, \quad a \rightarrow \frac{1}{\sqrt{c}}a \quad (2.15)$$

at fixed α . This results in the potentials

$$V(\phi_x) = -\alpha \log(b - \phi_x) - (2D - 1)(\alpha + 1) \log(a + c\phi_x) + [(2D - 1)cb - a]\phi_x \quad (2.16)$$

and

$$\tilde{V}(\phi) = -\alpha \log(b - \phi) + (\alpha + 1) \log(a + c\phi) - (a + cb)\phi. \quad (2.17)$$

It is easy to see that the potential (2.17) of the associated one-matrix model becomes the Penner one [16]

$$\tilde{V}_{Penner}(\phi) = -\alpha \log(b - \phi) - a\phi \quad (2.18)$$

as $c \rightarrow 0$.

2.2 One-cut solution

The one-cut solution for

$$E_\lambda \equiv \left\langle \frac{\text{tr}}{N} \left(\frac{1}{\lambda - \phi_x} \right) \right\rangle, \quad (2.19)$$

where the average is defined with the same measure as in (1.1), is given by the general formula [17]

$$E_\lambda = \int_{C_1} \frac{d\omega}{4\pi i} \frac{\tilde{V}'(\omega)}{(\lambda - \omega)} \frac{\sqrt{(\lambda - x_-)(\lambda - x_+)}}{\sqrt{(\omega - x_-)(\omega - x_+)}} \quad (2.20)$$

where the ends of the cut, x_\pm , are determined by the asymptotic conditions

$$\int_{C_1} \frac{d\omega}{2\pi i} \frac{\tilde{V}'(\omega)}{\sqrt{(\omega - x_-)(\omega - x_+)}} = 0, \quad \int_{C_1} \frac{d\omega}{2\pi i} \frac{\omega \tilde{V}'(\omega)}{\sqrt{(\omega - x_-)(\omega - x_+)}} = 2. \quad (2.21)$$

The contour C_1 encircles counterclockwise the cut leaving outside singularities of $\tilde{V}'(\omega)$ and the pole at $\lambda = \omega$ so that the integration over ω on the l.h.s. of Eq. (2.20) plays the role of a projector picking up negative powers of λ . It implies that the branch cut of E_λ does not pass through singularities (or branch cuts) of $\tilde{V}'(\lambda)$. This will be the case for our meromorphic $\tilde{V}'(\lambda)$, which has poles at $\lambda = -a$ and $\lambda = b$, providing they lie outside of the cut of E_λ .

For \tilde{V} given by (2.2) the contour integral can easily be calculated taking the residues at $\omega = \lambda, b$ and $-a$ while the residue at infinity vanishes since E_ω falls down as $1/\omega$. One gets

$$E_\lambda = \frac{1}{2} \left(\frac{\alpha}{b - \lambda} - a + \frac{\alpha + 1}{a + \lambda} - b \right) - \frac{1}{2} \sqrt{(\lambda - x_-)(\lambda - x_+)} \\ \cdot \left(\frac{|\alpha|}{b - \lambda} \frac{1}{\sqrt{(b - x_-)(b - x_+)}} - \frac{\alpha + 1}{a + \lambda} \frac{1}{\sqrt{(a + x_-)(a + x_+)}} \right) \quad (2.22)$$

where we use positive numerical values for $\sqrt{(b - x_-)(b - x_+)}$ and $\sqrt{(a + x_-)(a + x_+)}$ which are obtained from the analytic function $\sqrt{(\lambda - x_-)(\lambda - x_+)}$ whose cut is depicted

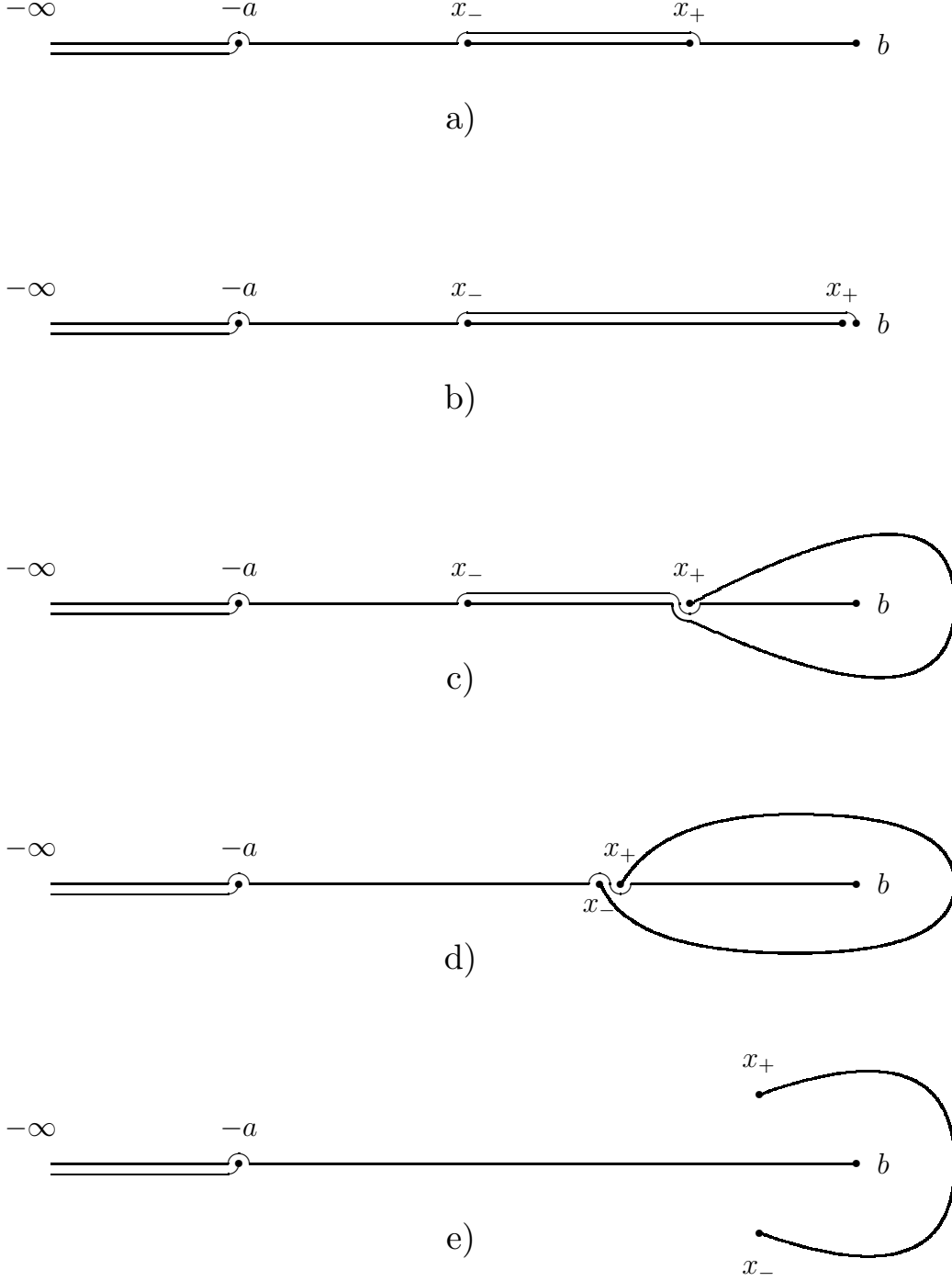


Figure 1: The eigenvalue support of the spectral density (the bold line) and the branch cuts of the logarithms (the thin lines): a) for $\alpha > 0$, b) for $\alpha \rightarrow +0$, c) for $-1 < \alpha < 0$, d) for $\alpha \rightarrow -1$ and e) for $\alpha < -1$.

for positive α in Figs. 1a), 1b) and for negative $-1 < \alpha < 0$ in Fig. 1c). When $\alpha \rightarrow -1$ from above, the point x_- approach x_+ along the real axis as is depicted in Fig. 1d). For $\alpha < -1$ the points x_- and x_+ become complex conjugate as is depicted in Fig. 1e).

Some comments concerning Eq. (2.22) and Fig. 1 are in order. In the Gaussian limit (2.11) Eq. (2.22) recovers the semicircle distribution of eigenvalues which has the support of the type depicted in Fig. 1a). The analytic function $\sqrt{(\lambda - x_-)(\lambda - x_+)}$ with this branch cut takes at $\lambda = b$ on the value

$$\sqrt{(\lambda - x_-)(\lambda - x_+)}\Big|_{\lambda=b} = \sqrt{(b - x_-)(b - x_+)} . \quad (2.23)$$

This solution realizes for all $\alpha > 0$.

When $\alpha \rightarrow +0$, the end of the cut, x_+ , approaches b as is depicted in Fig. 1b). For $\alpha < 0$ the boundary equations (2.21) were *not* have a solution for (2.23). For this reason the branch cut of the square root in Eqs. (2.20) and (2.21) should encircle the point b as is depicted in Fig. 1c) which provides

$$\sqrt{(\lambda - x_-)(\lambda - x_+)}\Big|_{\lambda=b} = -\sqrt{(b - x_-)(b - x_+)} . \quad (2.24)$$

Then the boundary equations (2.21) can be explicitly written as

$$\begin{aligned} \frac{|\alpha|}{\sqrt{(b - x_-)(b - x_+)}} &= a + \frac{1}{a + b} + \frac{x_- + x_+}{2} , \\ \frac{\alpha + 1}{\sqrt{(a + x_-)(a + x_+)}} &= b - \frac{1}{a + b} - \frac{x_- + x_+}{2} . \end{aligned} \quad (2.25)$$

They possess a solution both for positive and negative α .

Eq. (2.24) which is associated with the cut structure of Fig. 1c) is analogous to that for the Penner model [18] and for the generalized Penner model [19]. As is shown in the next subsection, the boundary equations (2.25) reduce to those for the Penner model under the rescaling (2.15) with $c \rightarrow 0$ at fixed α and the potential (2.17) smoothly interpolates between the Gaussian and Penner ones when α is decreased.

Eq. (2.24) always holds when the branch cut of the square root in Eqs. (2.20) and (2.21) encircles the point b and does not impose further restrictions on the location of the cut. It is convenient to take it along the support of the spectral density whose position in the complex plane is unambiguously determined by the criterion of Ref. [20]. The proper contour for $\alpha = -1$ is constructed in Appendix A.

2.3 Solution of the boundary equations

The boundary equations (2.25) can be conveniently rewritten introducing the variable

$$z = \frac{a - b}{2} + \frac{1}{a + b} + \frac{x_- + x_+}{2} \quad (2.26)$$

and shifting

$$\{\lambda, x_-, x_+\} = \{\hat{\lambda} + \frac{b-a}{2}, \hat{x}_- + \frac{b-a}{2}, \hat{x}_+ + \frac{b-a}{2}\} \quad (2.27)$$

which is analogous to (2.3). After this all quantities depend on α and β which is defined by Eq. (2.5) while the dependence on $a - b$ formally disappears from the equations. This was already discussed in Subsect. 2.1. In particular, Eq. (2.26) takes the form

$$z = \frac{1}{2\beta} + \frac{\hat{x}_- + \hat{x}_+}{2} \quad (2.28)$$

while Eqs. (2.25) read

$$\frac{|\alpha|}{\sqrt{(\beta - \hat{x}_-)(\beta - \hat{x}_+)}} = \beta + z, \quad \frac{\alpha + 1}{\sqrt{(\beta + \hat{x}_-)(\beta + \hat{x}_+)}} = \beta - z. \quad (2.29)$$

The product $\hat{x}_- \hat{x}_+$ can now be expressed via z by

$$\hat{x}_- \hat{x}_+ = \frac{1}{2} \left[\frac{\alpha^2}{(z + \beta)^2} + \frac{(\alpha + 1)^2}{(z - \beta)^2} \right] - \beta^2 \quad (2.30)$$

while z is determined via α and β by the 5th order algebraic equation

$$4\beta z - 2 = \frac{(\alpha + 1)^2}{(z - \beta)^2} - \frac{\alpha^2}{(z + \beta)^2} \quad (2.31)$$

which can be rewritten as

$$(\beta^2 - z^2)^2(4\beta z - 2) - (1 + 2\alpha)(\beta + z)^2 - 4\alpha^2\beta z = 0. \quad (2.32)$$

Finally, E_λ given by Eq. (2.22) takes the simple form

$$E_\lambda = \frac{1}{2} \left(\frac{\alpha}{\beta - \hat{\lambda}} + \frac{\alpha + 1}{\beta + \hat{\lambda}} \right) - \beta - \sqrt{(\hat{\lambda} - \hat{x}_-)(\hat{\lambda} - \hat{x}_+)} \frac{\beta(z + \hat{\lambda})}{\beta^2 - \hat{\lambda}^2}. \quad (2.33)$$

Eq. (2.32) is quadratic w.r.t. α . The two solutions read

$$\alpha_+ = (z + \beta)(\beta - z - \frac{1}{2z}) = \beta^2 - z^2 - \frac{\beta}{2z} - \frac{1}{2} \quad (2.34)$$

and

$$\alpha_- = (z + \beta)(z - \beta - \frac{1}{2\beta}) = z^2 - \beta^2 - \frac{z}{2\beta} - \frac{1}{2}. \quad (2.35)$$

It is easy to see from Eqs. (2.34) and (2.35) that

$$\begin{aligned} \alpha_+ + 1 &= (\beta - z)(\beta + z - \frac{1}{2z}) = \beta^2 - z^2 - \frac{\beta}{2z} + \frac{1}{2}, \\ \alpha_- + 1 &= (z - \beta)(z + \beta - \frac{1}{2\beta}) = z^2 - \beta^2 - \frac{z}{2\beta} + \frac{1}{2} \end{aligned} \quad (2.36)$$

so that Eq. (2.31) is obviously satisfied.

Then \hat{x}_\pm are determined from Eqs. (2.28) and (2.30) to be

$$\hat{x}_\pm|_{\alpha_+} = z - \frac{1}{2\beta} \pm \frac{\sqrt{(\beta^2 - z^2)(4\beta z - 1)}}{2\beta z} \quad (2.37)$$

and

$$\hat{x}_\pm|_{\alpha_-} = z - \frac{1}{2\beta} \quad (2.38)$$

for the solutions (2.34) and (2.35), respectively.

The solution (2.38) looks like a meromorphic one and not of the one-cut type. The spectral density has, nevertheless, a nontrivial support for this solution at some values of the parameters quite similarly for the solution (2.37) at $\alpha = -1$.⁴ The solution (2.38) can *not* be obtained, however, from the Gaussian case varying the parameters and the susceptibility (2.68) is strictly divergent at any values of the parameters α and β . We shall consider below for this reason only the solution (2.37) denoting α_+ just as α .

The equation (2.34) which determines z versus α and β is cubic and can be rewritten in the standard form

$$z^3 - z \left(\beta^2 - \alpha - \frac{1}{2} \right) + \frac{\beta}{2} = 0. \quad (2.39)$$

The discriminant of this equation is non-positive for

$$\alpha \leq \beta^2 - 3 \left(\frac{\beta}{4} \right)^{\frac{2}{3}} - \frac{1}{2}. \quad (2.40)$$

When the inequality (2.40) is satisfied, Eq. (2.39) possesses three real solutions. If the inequality (2.40) is not satisfied, then Eq. (2.39) has one real solution.

As we shall see in a moment the one-cut solution to our one-matrix model exists only in the domain of the parameters (2.40) where Eq. (2.39) has three real solutions. We choose the following one of them which is represented in a parametric form as

$$z = \frac{2}{\sqrt{3}} \sqrt{\beta^2 - \alpha - \frac{1}{2}} \cos \left(\frac{\pi}{6} + \frac{\theta}{3} \right), \quad \theta = \arcsin \left\{ \frac{\beta}{4} \left(\frac{1}{3} \left(\beta^2 - \alpha - \frac{1}{2} \right) \right)^{-\frac{3}{2}} \right\} \quad (2.41)$$

⁴For the solution (2.38) one gets

$$E_\lambda = \frac{1}{2} \left[\frac{\alpha}{\beta - \hat{\lambda}} + \frac{\alpha + 1}{\beta + \hat{\lambda}} \right] - \beta \pm \frac{1}{2} \left[\frac{\alpha}{\beta - \hat{\lambda}} + \frac{\alpha + 1}{\beta + \hat{\lambda}} + 2\beta \right] = \begin{cases} \frac{\alpha}{\beta - \hat{\lambda}} + \frac{\alpha + 1}{\beta + \hat{\lambda}} \\ -2\beta \end{cases}$$

and the support of the spectral density is along the closed contour C in the complex $\hat{\lambda}$ -plane which is determined by the equation

$$-2\beta\lambda + \alpha \log(\beta - \lambda) - (\alpha + 1) \log(\beta + \lambda) \Big|_{z - \frac{1}{2\beta}}^{\hat{\lambda}} = 0$$

with z given by the solution of the quadratic equation (2.35). The plus sign should be substituted outside of C and the minus sign should be substituted inside C .

and $0 \leq \theta \leq \frac{\pi}{2}$. The solution is well-defined in the domain of the parameters α and β restricted by the inequality (2.40) which is always satisfied for this solution while the equality sign corresponds to $\sin \theta = 1$. This solution is connected to the perturbative expansion around the Gaussian model when $\theta \rightarrow 0$.

In the Gaussian limit ($\alpha \sim \beta^2 \sim (\beta^2 - \alpha) \rightarrow \infty$) one gets from Eqs. (2.41), (2.37):

$$z = \sqrt{\beta^2 - \alpha}, \quad \frac{\hat{x}_+ - \hat{x}_-}{2} = \frac{\sqrt{\alpha}}{\sqrt{\beta} \sqrt[4]{\beta^2 - \alpha}}, \quad (2.42)$$

while (2.33) recovers the one for the semi-circle distribution with the parameter

$$\mu = \frac{2\beta}{\alpha} \sqrt{\beta^2 - \alpha}. \quad (2.43)$$

μ exists for $\alpha < \beta^2$ and vanishes at $\alpha = \beta^2$ which exactly coincides with the criterion based on (2.40).

The limit of the cubic potential is described by the solution (2.41) when $\alpha \rightarrow \infty$ in the vicinity of β^2 as $\beta \rightarrow \infty$ so that

$$\beta^2 - \alpha \sim \beta^{\frac{2}{3}}. \quad (2.44)$$

No simplifications occurs in this limit in (2.41) and (2.40) which recover the known results for the cubic potential [21].

In the Penner limit ($\beta \rightarrow \infty$, $\alpha \sim 1$) Eqs. (2.41) and (2.37) yields

$$z = \beta - \frac{\alpha + 1}{2\beta}, \quad \frac{\hat{x}_- - \hat{x}_+}{2} = \frac{\sqrt{\alpha + 1}}{\beta} \quad (2.45)$$

and Eq. (2.33) recovers the solution for the Penner model. The inequality (2.40) is always satisfied.

The proper regions of the parameters are depicted in Fig. 2. The bold line which starts at $\alpha = \beta = 0$ corresponds to the equality sign in (2.40). The solution (2.41) is well-defined below this line.

2.4 The critical behavior

The critical behavior of our model can emerge when:

- i) The spectral density ceases to be positive at the interval $[\hat{x}_-, \hat{x}_+]$ as for the one-matrix models with a polynomial potential.
- ii) Either \hat{x}_- approaches $-\beta$ or \hat{x}_+ approaches β .
- iii) \hat{x}_- approaches \hat{x}_+ like for the Penner model [22].

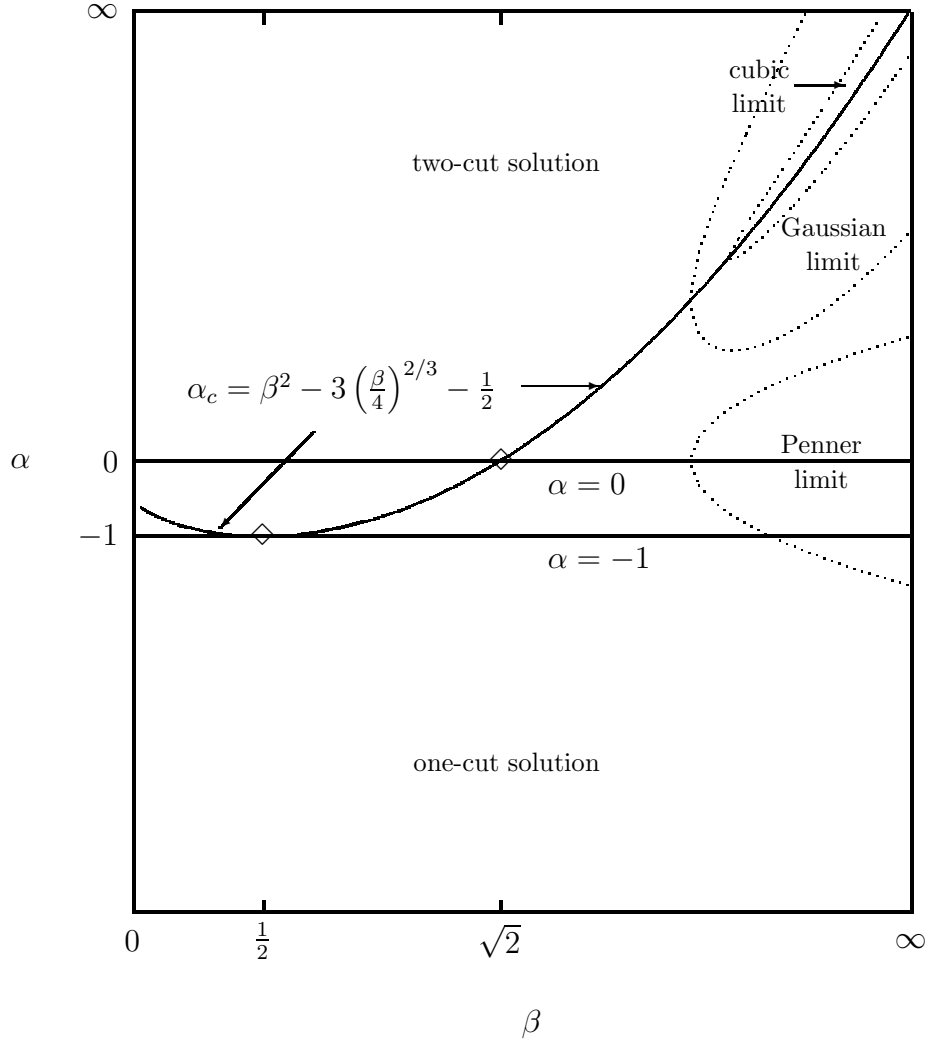


Figure 2: The phase diagram of the Kazakov–Migdal model with the potential (2.1). The one-cut solution realizes for $\alpha < \alpha_c$. The critical lines $\alpha = \alpha_c$ and $\alpha = -1$ correspond to $\gamma_{str} = -1/2$ and $\gamma_{str} = 0$, respectively, while the tri-critical point $\beta = 1/2$, $\alpha = -1$ is associated with the Kosterlitz–Thouless phase transition.

Since we start from the Gaussian solution, we shall verify that a phase transition of the type *i*), which restricts the one-cut solution, does not occur before those of the type *ii*) or *iii*). The proper criterion can be obtained from Eq. (2.33) where the factor $z + \hat{\lambda}$ should vanish for some $\hat{\lambda} \in [\hat{x}_-, \hat{x}_+]$ for this phase transition to occur. The equation for the critical points associated with $\hat{x}_- = -z$ can be easily obtained from Eq. (2.37). It has the following solution for the critical value of α at given β

$$\hat{x}_- = -z \quad \text{for} \quad \alpha_c = \beta^2 - 3 \left(\frac{\beta}{4} \right)^{\frac{2}{3}} - \frac{1}{2} \quad (2.46)$$

which exactly coincides with equality sign in (2.40) when the discriminant of the cubic equation (2.39) vanishes. For this reason the inequality $\hat{x}_- > -z$ which means the existence of the one-cut solution (2.33) is equivalent to (2.40). This is why the expression (2.41) fully describes our one-cut solution of the one-matrix model.

It is easy to understand why the critical value (2.46) is associated with the vanishing of the discriminant. We can identically rewrite Eq. (2.39) as

$$\alpha_c - \alpha = \left(z - \left(\frac{\beta}{4} \right)^{\frac{1}{3}} \right)^2 \left(1 + \frac{2}{z} \left(\frac{\beta}{4} \right)^{\frac{1}{3}} \right) \quad (2.47)$$

which looks like the genus zero string equation in polynomial one-matrix models [23]. For the critical behavior to occur, two roots of the cubic equation should coincide which happens when the discriminant vanishes. The critical value of z extracted from Eq. (2.47) is

$$z_c = \left(\frac{\beta}{4} \right)^{\frac{1}{3}} \quad (2.48)$$

and near the critical point

$$\alpha_c - \alpha = (z - z_c)^2 \left(1 + \frac{2z_c}{z} \right) \approx 3(z - z_c)^2 \quad (2.49)$$

in the full analogy to one-matrix models with polynomial potentials.

It follows also from the above formulas that z given by Eq. (2.41) is a monotone function of both α and β in the region where the inequality (2.40) is satisfied since

$$\frac{\partial \alpha}{\partial z} = \frac{2}{z^2} (z_c^3 - z^3) \quad (2.50)$$

and

$$\frac{\partial \beta}{\partial z} = \frac{z^3 - z_c^3}{z^2 \sqrt{z^2 + \alpha + \frac{1}{2} + \frac{1}{16z^2}}} \quad (2.51)$$

while $z \geq z_c$ in the domain (2.40). The expression under the square root in the latter formula is always non-negative for $\alpha \geq -1$.

Another set of singular points is when $\hat{x}_+ = \beta$. From Eq. (2.37) we find that this happens for z given by Eq. (2.41) only when $\alpha = 0$:

$$\hat{x}_+ = \beta \quad \text{for} \quad \alpha = 0, \quad (2.52)$$

while z is expressed via β along the line $\alpha = 0$ by

$$z = \frac{\beta}{2} + \sqrt{\frac{\beta^2}{4} - \frac{1}{2}} \quad \text{for} \quad \alpha = 0. \quad (2.53)$$

Eq. (2.53) is applicable for $\beta \geq \beta_c = \sqrt{2}$. The value $\beta_c = \sqrt{2}$ satisfies Eq. (2.46) at $\alpha = 0$. Therefore, the critical line (2.52) which is depicted in Fig. 2 by the solid line terminates at the intersection with the critical line (2.46). The tri-critical point is given by

$$\alpha_c = 0, \quad \beta_c = \sqrt{2}. \quad (2.54)$$

Analogously, \hat{x}_- and \hat{x}_+ coincide for the solution (2.41) when $\alpha = -1$:

$$\hat{x}_- = \hat{x}_+ \quad \text{for} \quad \alpha = -1, \quad (2.55)$$

while z is expressed via β along the line $\alpha = -1$ by

$$z = \beta \quad \text{for} \quad \alpha = -1. \quad (2.56)$$

Eq. (2.56) is applicable for $\beta \geq \beta_c = 1/2$. The value $\beta_c = 1/2$ satisfies Eq. (2.46) at $\alpha = -1$. Therefore, the critical line (2.55) which is depicted in Fig. 2 by the solid line terminates at the intersection with the critical line (2.46). The corresponding tri-critical point reads

$$\alpha_c = -1, \quad \beta_c = \frac{1}{2}. \quad (2.57)$$

Note that the critical lines (2.52) and (2.55) lie in the allowed region below the line (2.46).

2.5 Calculation of susceptibility

The critical behavior of the model (1.1) with the potential (2.1) is characterized by the susceptibility

$$\chi \equiv -\frac{1}{N^2 \text{Vol.}} \frac{d^2}{d\alpha^2} \log Z \quad (2.58)$$

where Vol. stands for the volume of the system

$$\text{Vol.} = \sum_x 1. \quad (2.59)$$

By differentiating (1.1) one gets explicitly

$$\begin{aligned} \chi = & -\frac{d}{d\alpha} \left\langle \frac{\text{tr}}{N} [\log(b - \phi_x) + (2D - 1) \log(a + \phi_x)] \right\rangle = \\ & - \oint_{C_1} \frac{d\omega}{2\pi i} [\log(b - \omega) + (2D - 1) \log(a + \omega)] \dot{E}_\omega \end{aligned} \quad (2.60)$$

where

$$\dot{E}_\omega \equiv \frac{dE_\omega}{d\alpha}. \quad (2.61)$$

Compressing the contour C_1 in Eq. (2.60) to the cuts of the logarithms, one gets

$$\chi = - \left\{ \int_{-\infty}^b dt \dot{E}_t + (2D-1) \int_{-\infty}^{-a} dt \dot{E}_t \right\}. \quad (2.62)$$

This formula can alternatively be derived from (2.60) using the identities

$$\frac{d}{d\alpha} \left\langle \frac{\text{tr}}{N} \log(b - \phi_x) \right\rangle = \frac{d}{d\alpha} \int_{-\infty}^b dt \left\langle \frac{\text{tr}}{N} \frac{1}{(t - \phi_x)} \right\rangle = \int_{-\infty}^b dt \dot{E}_t \quad (2.63)$$

and

$$\frac{d}{d\alpha} \left\langle \frac{\text{tr}}{N} \log(a + \phi_x) \right\rangle = \frac{d}{d\alpha} \int_{-\infty}^{-a} dt \left\langle \frac{\text{tr}}{N} \frac{1}{(t - \phi_x)} \right\rangle = \int_{-\infty}^{-a} dt \dot{E}_t. \quad (2.64)$$

To calculate χ in genus zero, we use the formula

$$\dot{E}_\lambda = \int_{C_1} \frac{d\omega}{4\pi i} \frac{\dot{\tilde{V}}'(\omega)}{(\lambda - \omega)} \frac{\sqrt{(\omega - x_-)(\omega - x_+)}}{\sqrt{(\lambda - x_-)(\lambda - x_+)}} \quad (2.65)$$

which can be proven by a direct differentiation of Eqs. (2.20) and (2.21) and holds for the derivative w.r.t. *any* parameter of the potential \tilde{V} , in particular w.r.t. α . For our logarithmic potential (2.2) one gets explicitly

$$\begin{aligned} \dot{E}_\lambda = \frac{1}{2} & \left\{ \frac{1}{b - \lambda} + \frac{1}{a + \lambda} + \frac{1}{\sqrt{(\lambda - x_-)(\lambda - x_+)}} \right. \\ & \times \left[\pm \frac{\sqrt{(b - x_-)(b - x_+)}}{\lambda - b} + \frac{\sqrt{(a + x_-)(a + x_+)}}{\lambda + a} \right] \Big\}. \end{aligned} \quad (2.66)$$

Here and below the plus sign in front of the first term in the square brackets is associated with $\alpha > 0$ while the minus sign corresponds to $\alpha < 0$. The result of Ref. [19] for the generalized Penner model is recovered by this formula as $a \rightarrow \infty$.

The integral in Eq. (2.62) with \dot{E}_t given by (2.66) is easily calculable using the following formula for an indefinite integral

$$\int dt \dot{E}_t = \frac{1}{2} \log \left\{ \frac{\left(\sqrt{(t - x_-)(a + x_+)} + \sqrt{(t - x_+)(a + x_-)} \right)^2}{\left(\sqrt{(t - x_-)(b - x_+)} \pm \sqrt{(t - x_+)(b - x_-)} \right)^2} \right\} \quad (2.67)$$

which yields for the susceptibility in genus zero

$$\begin{aligned} \chi_0 = (D-1) \log & \left\{ \frac{1}{4} \left(\sqrt[4]{\frac{(a + x_-)(b - x_+)}{(a + x_+)(b - x_-)}} \pm \sqrt[4]{\frac{(a + x_+)(b - x_-)}{(a + x_-)(b - x_+)}} \right)^2 \right\} + \\ & D \log \left\{ \left(\sqrt[4]{\frac{(a + x_-)}{(a + x_+)}} + \sqrt[4]{\frac{(a + x_+)}{(a + x_-)}} \right)^2 \right\} - D \log \left\{ \left(\sqrt[4]{\frac{(b - x_+)}{(b - x_-)}} \pm \sqrt[4]{\frac{(b - x_-)}{(b - x_+)}} \right)^2 \right\}. \end{aligned} \quad (2.68)$$

As before the positive sign in \pm corresponds to $\alpha > 0$ while the minus sign should be substituted for $\alpha < 0$. As is already mentioned in the previous subsection, the $\alpha < 0$ case can be obtained from the $\alpha > 0$ case by changing the sign of $\sqrt{(b - x_-)(b - x_+)}$.

Let us briefly discuss some properties of the expression (2.68) which will be used in the next section for studying the continuum limits of our model. If $\alpha > 0$ the contour of integrations over t , which coincide with the branch cuts of the logarithms depicted in Fig. 1a), can be moved along the complex plane. In particular, one can integrate in the first term on the r.h.s. of Eq. (2.62) from b to $+\infty$ along the positive real axis. The result is the same and is not singular at $x_- = x_+$ if one substitutes the plus sign in Eq. (2.68).

On the contrary, the points x_- and x_+ can pinch the integration contour for $\alpha < 0$ as is depicted in Fig. 1d) for $\alpha = -1$. This results in a logarithmic singularity of (2.68) at $x_- = x_+$ when one substitutes the minus sign in Eq. (2.68):

$$\chi_0 \approx -\log(x_- - x_+)^2. \quad (2.69)$$

An analogous logarithmic singularity emerges when $x_+ \approx b$ as is depicted in Fig. 1b) at $\alpha \approx 0$:

$$\chi_0 \approx \log(b - x_+). \quad (2.70)$$

Note, that

$$\chi_0 = -\log(1 + \alpha) + \log \alpha \quad (2.71)$$

in the Penner limit (2.15) with $c \rightarrow 0$ when x_{\pm} are given by

$$x_{\pm} = b - \frac{\alpha + 2}{a} \pm \frac{2}{a} \sqrt{\alpha + 1}. \quad (2.72)$$

Eq. (2.71) coincides with the susceptibility for the Penner model [22] and recovers the singularities (2.69) and (2.70).

Having the explicit formula (2.68) for χ_0 , we can find out which γ_{str} is associated with each type of the critical behavior (2.46), (2.52) and (2.55). Along the line (2.46) where χ_0 is not singular and equals to some value χ_0^c , one gets

$$\chi_0 - \chi_0^c \sim (x_- - x_-^c). \quad (2.73)$$

Since $(x_- - x_-^c) \sim (\alpha_c - \alpha)^{1/2}$ near the critical line (2.46), one obtains $\gamma_{str} = -1/2$.

Near the critical lines (2.52) and (2.55), where χ_0 is given by Eqs. (2.69) and (2.70), one gets $\gamma_{str} = 0$. While (2.69) is positive, (2.70) is negative. For this reason we shall not consider the continuum limit associated with the critical line (2.52) as well as the tri-critical point (2.54) since it corresponds to a negative susceptibility. The susceptibility in the vicinity of the tri-critical point (2.57) is considered in Subsect. 3.3.

3 The continuum limits

The continuum theories are obtained by an expansion near the critical points. The continuum limit associated with $\gamma_{str} = 0$ describes in a standard way $2D$ gravity plus $1D$ critical

matter. The continuum limit associated with $\gamma_{str} = -1/2$ looks like pure $2D$ gravity for local observables which are defined at the same site of the lattice. For another type of observables — extended Wilson loops — the continuum limit sets up at distances $L \sim 1/\sqrt{\varepsilon}$ with ε being a deviation from the critical point. This is due to a singular behavior of the Itzykson–Zuber correlator of gauge fields for this phase. A Kosterlitz–Thouless phase transition separates the two phases.

3.1 $\gamma_{str} = -1/2$

In order to find out what kind of continuum theory is associated with the critical behavior (2.46), let us expand all quantities near the edge singularity of the spectral density substituting

$$z = z_c + \varepsilon\sqrt{\Lambda}, \quad z_c = \left(\frac{\beta}{4}\right)^{\frac{1}{3}} \quad (3.1)$$

where $\varepsilon \rightarrow 0$ and Λ is to be identified with the cosmological constant of $2D$ gravity. From Eqs. (2.47), (2.37) one gets

$$\alpha_c - \alpha = 3\varepsilon^2\Lambda, \quad \hat{x}_- = -z_c + 2\varepsilon\sqrt{\Lambda}, \quad \hat{x}_+ = 3z_c - \frac{1}{\beta}. \quad (3.2)$$

Introducing the continuum momentum variable, ξ , by

$$\hat{\lambda} = -z_c + \varepsilon\xi \quad (3.3)$$

one gets from Eq. (2.33)

$$E_\lambda = -\frac{1}{2z_c} + \varepsilon\xi - \varepsilon^{3/2}(\xi + \sqrt{\Lambda})\sqrt{-\xi + 2\sqrt{\Lambda}}\frac{2}{\sqrt{z_c}\sqrt{16z_c^4 - 1}} + \mathcal{O}(\varepsilon^2). \quad (3.4)$$

The last term on the r.h.s. determines the continuum spectral density

$$\rho_c(\xi) = \frac{1}{\pi}(\xi + \sqrt{\Lambda})\sqrt{\xi - 2\sqrt{\Lambda}} \quad (3.5)$$

and, therefore, all continuum correlators of the trace of powers of the (renormalized) field $\Phi(x)$ at some point x , which is the standard set of observables of $2D$ gravity.

While the gravitational part of the system is continuous, this does not necessarily mean that matter becomes critical. An example is the Ising model on a random lattice where it is easy to construct the $\gamma_{str} = -1/2$ behavior which is associated with continuum $2D$ gravity and non-critical matter while matter becomes critical at a tri-critical point changing the value of the string susceptibility to $\gamma_{str} = -1/3$.

A direct way to verify whether matter becomes critical at a given fixed point is to investigate observables which are associated with extended objects — the open-loop averages

$$G_{\nu\lambda}(C_{xy}) = \left\langle \frac{\text{tr}}{N} \left(\frac{1}{\nu - \phi_x} U(C_{xy}) \frac{1}{\lambda - \phi_y} U^\dagger(C_{xy}) \right) \right\rangle, \quad (3.6)$$

where C_{xy} goes from x to y along some path on a D -dimensional lattice and the average is w.r.t. the same measure as in (1.1). $G_{\nu\lambda}(C_{xy})$ is symmetric in ν and λ due to invariance of the Haar measure, dU , under the transformation $U \rightarrow U^\dagger$.

The averages (3.6) depend [24] at large N only on the algebraic length $L(C_{xy})$ of the contour C_{xy} (*i.e.* the one after contracting backtrackings) and can be calculated [25] providing $C(\nu, \lambda)$ — the one-link Itzykson–Zuber correlator of the gauge fields — is known. The latter is expressed via the double discontinuity of

$$G_{\nu\lambda} \equiv G_{\nu\lambda}(1) \quad (3.7)$$

across the cut:

$$C(\nu, \lambda) \equiv \frac{1}{\pi^2 \rho(\nu) \rho(\lambda)} \text{Disc}_\nu \text{Disc}_\lambda G_{\nu\lambda}, \quad (3.8)$$

where the continuous and discontinuous in ν parts of $G_{\nu\lambda}$ are defined by

$$\begin{aligned} \text{Disc}_\nu G_{\nu\lambda} &\equiv \frac{G_{(\nu+i0)\lambda} - G_{(\nu-i0)\lambda}}{2i}, \\ \text{Cont}_\nu G_{\nu\lambda} &\equiv \frac{G_{(\nu+i0)\lambda} + G_{(\nu-i0)\lambda}}{2} \end{aligned} \quad (3.9)$$

so that for a real λ outside of the cut (cuts) $\text{Disc}_\nu G_{\nu\lambda}$ coincides with the imaginary part and $\text{Cont}_\nu G_{\nu\lambda}$ coincides with the real part. In particular, $\text{Disc}_\nu E_\nu = -i\pi\rho(\nu)$.

For the potential (2.1) $G_{\nu\lambda}$ reads [7]

$$G_{\nu\lambda} = \frac{(b - \nu)E_\nu - (a + \lambda)E_\lambda + 1}{(\lambda + a + E_\nu)(b - \nu) - \alpha}. \quad (3.10)$$

The few lower terms of the expansion of $G_{\nu\lambda}$ in ε are

$$G_{\nu\lambda} = \frac{2}{4z_c^2 + 1} - i\pi\sqrt{\varepsilon} \frac{\rho_c(\xi_\nu) - \rho_c(\xi_\lambda)}{\nu - \lambda} \frac{(4z_c^2 - 1)}{(4z_c^2 + 1)} + \mathcal{O}(\varepsilon) \quad (3.11)$$

which is similar to the one in a two-matrix model [15]. The double discontinuity of the first two terms on the r.h.s. vanishes so that one needs the term at least $\mathcal{O}(\varepsilon)$.

For this reason we start directly from the exact $C(\nu, \lambda)$ which for the potential (2.1) reads [7]

$$C(\nu, \lambda) = \frac{a + \lambda}{(b - \nu)[\lambda - r_+(\nu)][\lambda - r_-(\nu)]} \quad (3.12)$$

where

$$r_\pm(\lambda) = \frac{1}{2} \left\{ \frac{\alpha}{b - \lambda} - \frac{\alpha + 1}{a + \lambda} + b - a \right\} \pm i\pi\rho(\lambda). \quad (3.13)$$

The r.h.s. of Eq. (3.12) is symmetric in ν and λ due to the relation

$$r_\pm(r_\mp(\lambda)) = \lambda \quad (3.14)$$

which is satisfied by the solution (2.22) [8]. Analogously to Ref. [4], it is easy to see that Eq. (3.14) is satisfied by our explicit continuum formulas.

To calculate the continuum limit of (3.12), we expand

$$r_{\pm}(\lambda) = -z_c + \varepsilon\xi - \frac{3\varepsilon^2\xi^2}{z_c(16z_c^4 - 1)} + \mathcal{O}(\varepsilon^3) \pm i\pi\rho(\lambda). \quad (3.15)$$

We put here $\Lambda = 0$ and keep terms of order ε^2 which we shall need below. One gets

$$C(\nu, \lambda) = \frac{1}{\varepsilon^2} \frac{(4z_c^2 - 1)}{(4z_c^2 + 1)} \frac{(1 + \varepsilon \frac{\xi_\nu}{z_c(4z_c^2 - 1)})(1 + \varepsilon \frac{\xi_\lambda}{z_c(4z_c^2 - 1)})}{(\xi_\nu - \xi_\lambda)^2 + \frac{2\varepsilon\xi_\nu\xi_\lambda(\xi_\nu + \xi_\lambda)}{z_c(16z_c^4 - 1)}}. \quad (3.16)$$

This expression comes from the $\mathcal{O}(\varepsilon)$ term in the expansion (3.11) since the denominator in (3.8) is $\mathcal{O}(\varepsilon^3)$.

In the continuum limit $\varepsilon = 0$ we get from Eq. (3.16)

$$C_c(x, y) \propto \frac{1}{(x - y)^2} \quad (3.17)$$

which coincides with $C(x, y)$ for the quadratic potential [25]⁵

$$C(x, y) = \frac{\sqrt{\mu^2 + 4} + \mu}{2(x^2 - \sqrt{\mu^2 + 4}xy + y^2 + \mu)} \quad (\text{quadratic potential}) \quad (3.18)$$

at $\mu = 0$. While for the quadratic potential $\mu = 0$ is possible only at $D = 1$ where it is associated with the naive continuum limit [6], Eq. (3.17) holds in our case at any D along the line (2.46).

The expression (3.18) for the Gaussian $C(x, y)$ possesses a remarkable convolution property [26] — keeps its functional structure when one combines the path of the length $L_1 + L_2$ from the paths of the lengths L_1 and L_2 . Then

$$C(x, y; L_1 + L_2) = \int dt \rho(t) C(x, t; L_1) C(t, y; L_2) \quad (3.19)$$

where

$$C(\nu, \lambda; L) \equiv \frac{1}{\pi^2 \rho(\nu) \rho(\lambda)} \text{Disc}_\nu \text{Disc}_\lambda G_{\nu\lambda}(C_{xy}). \quad (3.20)$$

Observables which are associated with matter reveal singularities at $\mu = 0$ and become finite after an appropriate renormalization.

Since our expression (3.17) looks like the Gaussian one for $\mu = 0$, one might expect a similar property of matter correlators. However, when (3.17) is substituted into Eq. (3.19), the integral is divergent at $t = x$ or $t = y$. To regularize, we keep $\mathcal{O}(\varepsilon)$ term in the denominator of (3.16). Now the integral is $\mathcal{O}(\varepsilon^{-1/2})$ which exactly cancels an extra $\mathcal{O}(\varepsilon^{1/2})$ factor which emerges since each of two C in the integral (3.19) is proportional to $1/\varepsilon^2$ (according to Eq. (3.16)) and the measure is proportional to $\varepsilon^{5/2}$. Therefore, one gets

$$C(x, y; 2) \propto \frac{1}{\varepsilon^2(x - y)^2} \quad (3.21)$$

⁵An analogous formula for the two-matrix model has been earlier obtained in Ref. [14].

and the functional structure of C_c is preserved. The coefficient of proportionality is calculated below.

An interesting question is whether Eq. (3.19) with ρ given by the continuum formula (3.5) can have a solution with the same functional structure for macroscopic loops as well. A solution to this equation for $\Lambda = 0$ is given by

$$C_c(x, y; \sqrt{u}) = \frac{2\sqrt{u}}{(x-y)^2 + 2u(x+y)xy + u^2x^2y^2} \quad (3.22)$$

which obeys the following convolution property

$$\frac{1}{\pi} \int_0^\infty dt t^{\frac{3}{2}} C_c(x, t; \sqrt{u}) C_c(t, y; \sqrt{v}) = C_c(x, y; \sqrt{u} + \sqrt{v}). \quad (3.23)$$

This formula is proven in Appendix B.

It is easy to see that the solution (3.22) satisfies the initial condition (3.17) for $u \rightarrow 0$. To find the relation between u and the length L , let us first rescale

$$\xi \rightarrow \xi \frac{\sqrt{z_c(16z_c^4 - 1)}}{2}, \quad u \rightarrow u \frac{\sqrt{z_c(16z_c^4 - 1)}}{2}. \quad (3.24)$$

Now the denominator in (3.22) coincides to order ε with the one in (3.16) providing

$$u = \frac{\varepsilon}{4}. \quad (3.25)$$

It follows then from Eq. (3.23) that

$$u = L^2 \frac{\varepsilon}{4} \quad (3.26)$$

where the length L is measured in the lattice units.

One sees from Eqs. (3.22) and (3.26) that the continuum limit of extended correlators is reached at distances

$$L \sim \frac{1}{\sqrt{\varepsilon}} \quad (3.27)$$

rather than $\sim 1/\varepsilon$ as it might be naively expected. Therefore, a nontrivial scale dimension of the matter field is developed at macroscopic distances.

The knowledge of the L -dependence of C_c allows us to calculate correlators of extended objects. The simplest one is that of the adjoint Wilson loop

$$W_A(C) \equiv \left\langle \left(\left| \frac{\text{tr}}{N} U(C) \right|^2 - 1 \right) \right\rangle = \frac{1}{N^2} \int dt \rho(t) C(t, t; L). \quad (3.28)$$

Substituting (3.22), one gets

$$W_A(C) = \frac{2\sqrt{u}}{\varepsilon\pi} \int_0^\infty \frac{dt t^{3/2}}{4ut^3 + u^2t^4} = -\frac{1}{4\varepsilon}. \quad (3.29)$$

Since the integral is divergent as $t \rightarrow 0$, the result is obtained by an analytic continuation. This divergence might be related to the fact that we put $\Lambda = 0$.

Note, that the correlator (3.29) is divergent when $\varepsilon \rightarrow 0$ similarly to the one for the Gaussian case [26] as $\mu \rightarrow 0$. One concludes, therefore, that matter could become critical at distances (3.27). This mechanism does *not* work for the two-matrix model which is associated with $D = 1/2$ in the above formulas. In order to have $L \rightarrow \infty$ as $\varepsilon \rightarrow 0$, one needs $D \geq 1$. For $D = 1$ one should choose a closed matrix chain since otherwise the gauge field can be absorbed by a gauge transformation of ϕ_x .

Analogously to (3.29) one can calculate the more general correlator

$$G_\lambda(C) \equiv \left\langle \frac{\text{tr}}{N} \left(\frac{1}{\lambda - \phi_x} U(C_{xx}) \right) \frac{\text{tr}}{N} U^\dagger(C) \right\rangle = \frac{1}{N^2} \int dt \rho(t) C(t, t; L) \frac{1}{\lambda - t}. \quad (3.30)$$

In the continuum limit one gets

$$G_\xi(C) = \frac{2\sqrt{u}}{\varepsilon^2 \pi} \int_0^\infty \frac{dt t^{3/2}}{(4ut^3 + u^2 t^4)} \frac{1}{(\xi - t)} = \frac{1}{2\varepsilon^2 \sqrt{u}} \left\{ \frac{(-\xi)^{-3/2} - \left(\frac{u}{4}\right)^{3/2}}{1 + \frac{\xi u}{4}} \right\}. \quad (3.31)$$

This expression is also divergent when $\varepsilon \rightarrow 0$.

Finally, the continuum part of $G_{\nu\lambda}(C)$ is given by

$$\begin{aligned} G_{\zeta\xi}(C) &= 2\sqrt{\varepsilon u} \frac{1}{\pi} \int_0^\infty dx dy \frac{x^{3/2} y^{3/2}}{(x-y)^2 + 2u(x+y)xy + u^2 x^2 y^2} \frac{1}{(\zeta-x)(\xi-y)} \\ &= 2\sqrt{\varepsilon u} \frac{(-\zeta)^{3/2} (-\xi)^{3/2}}{(\zeta-\xi)^2 + 2u(\zeta+\xi)\zeta\xi + u^2 \zeta^2 \xi^2} + \dots \end{aligned} \quad (3.32)$$

This expression is indeed $\mathcal{O}(\varepsilon)$ for $L \sim 1$ in agreement with (3.11) while it is $\mathcal{O}(\sqrt{\varepsilon})$ for $L \sim 1/\sqrt{\varepsilon}$.

3.2 $\gamma_{str} = 0$

Another continuum limit is associated with the critical line $\alpha = -1$. One substitutes the expansion near the edge singularity which is quite similar to the one for the Penner model [18]. Introducing the cosmological constant, Λ , by

$$\alpha = -1 + \varepsilon^2 \Lambda \beta^2 \quad (3.33)$$

where an extra factor is inserted for a latter convenience, we get from Eq. (2.41)

$$z = \beta - \frac{8\varepsilon^2 \beta^3}{4\beta^2 - 1} \Lambda \quad (3.34)$$

and from Eq. (2.37)

$$\hat{x}_\pm = \beta - \frac{1}{2\beta} \pm 2\varepsilon \sqrt{\Lambda}. \quad (3.35)$$

Defining the continuum momentum ξ by

$$\hat{\lambda} = \beta - \frac{1}{2\beta} + \varepsilon\xi, \quad (3.36)$$

one gets from Eq. (2.33)

$$E_\lambda = -2\beta - 2\beta^2\varepsilon\xi - \varepsilon\sqrt{\xi^2 - 4\Lambda}2\beta^2 + \mathcal{O}(\varepsilon^2) \quad (3.37)$$

which determines the continuum spectral density to be

$$\rho_c(\xi) = \frac{1}{\pi}\sqrt{\xi^2 - 4\Lambda}. \quad (3.38)$$

The one-link Itzykson–Zuber correlator (3.12) reads

$$C(\nu, \lambda) = \frac{4\beta^2}{4\beta^2 - 1} + \mathcal{O}(\varepsilon). \quad (3.39)$$

This expression does not depend on the continuum momenta ξ_ν and ξ_λ similar to the Gaussian expression (3.18) for $x, y \ll 1$. Thus, nothing special happens with the Itzykson–Zuber correlators in the $\gamma_{str} = 0$ continuum limit far away from the tri-critical point in contrast to the $\gamma_{str} = -1/2$ case.

3.3 Kosterlitz–Thouless phase transition

The above formulas are not applicable in the vicinity of the tri-critical point $\beta_c = 1/2$, $\alpha_c = -1$ where the continuum system undergoes a Kosterlitz–Thouless phase transition, which was previously studied for a closed matrix chain [27, 28], between the phases with $\gamma_{str} = -1/2$ and $\gamma_{str} = 0$. This domain is most interesting and should be treated separately.

Let us expand

$$\beta = \frac{1}{2} + \delta\beta, \quad \alpha = -1 + \delta\alpha, \quad z = \frac{1}{2} + \delta z, \quad \lambda = -\frac{1}{2} + \delta\lambda. \quad (3.40)$$

Then for the solution (2.41) one gets

$$\delta z = \frac{1}{3}\delta\beta + \sqrt{\frac{4}{9}(\delta\beta)^2 - \frac{1}{3}\delta\alpha} \quad (3.41)$$

while the inequality (2.40) reduces to

$$\delta\alpha \leq \frac{4}{3}(\delta\beta)^2. \quad (3.42)$$

It is convenient to parametrize the vicinity of the tri-critical point by the lines

$$\delta\alpha = (3\kappa + 1)(1 - \kappa)(\delta\beta)^2 \quad (3.43)$$

which obey the inequality (3.42) for any κ . We choose $1/3 \leq \kappa \leq 1$ where the factor in Eq. (3.43) is a monotone function of κ . The cases $\kappa = 1/3$ and $\kappa = 1$ are associated with the critical lines (2.46) and (2.55), respectively. Then, (3.41) is rewritten as

$$\delta z = \kappa \delta \beta \quad (3.44)$$

while Eq. (2.37) gives

$$\hat{x}_{\pm} = -\frac{1}{2} + (2 + \kappa)\delta\beta \pm 2\sqrt{2(1 - \kappa^2)}\delta\beta. \quad (3.45)$$

Eqs. (3.43), (3.44), (3.45) recover Eqs. (3.1), (3.2) or Eqs. (3.33), (3.34) (3.35) if

$$\kappa = \frac{1}{3} + \frac{\varepsilon\sqrt{\Lambda}}{\delta\beta} \quad (3.46)$$

or

$$\kappa = 1 - \frac{\varepsilon^2\Lambda}{4(\delta\beta)^2} \quad (3.47)$$

with $\varepsilon \ll \delta\beta$, respectively.

The susceptibility (2.68) can easily be expressed via $\delta\beta$ and κ near the tri-critical point:

$$\chi_0 = -\log\left(\frac{1 - \kappa}{1 + 3\kappa}\right) - 2D \log(\sqrt{2}\delta\beta). \quad (3.48)$$

The first term on the r.h.s. recovers Eq. (2.69) in the limit (3.47) while the second one which becomes singular when $\delta\beta \rightarrow 0$ is a new type of singularity which appears only at the tri-critical point. Notice that this second term is D dependent. Using Eq. (3.43) one can rewrite (3.48) alternatively via $\delta\alpha$.

The continuum spectral density can be obtained from (2.33) by substituting the expansions (3.44) and (3.45) which gives

$$\rho_c(\delta\lambda) = \frac{1}{2\pi} \sqrt{(\delta\lambda - (2 + \kappa)\delta\beta)^2 - 8(1 - \kappa^2)(\delta\beta)^2} \frac{\kappa\delta\beta + \delta\lambda}{\delta\beta + \delta\lambda}. \quad (3.49)$$

For $\kappa > 1/3$ the zeros both of the numerator and of the denominator lie outside of the eigenvalue support. In the limits (3.46) and (3.47) this expression recover Eqs. (3.5) and (3.38), respectively.

The one-link Itzykson–Zuber correlator (3.12) near the tri-critical point reads

$$C(\delta\nu, \delta\lambda) = \frac{(\delta\lambda + \delta\beta)(\delta\nu + \delta\beta)}{\mathcal{D}(\delta\nu, \delta\lambda)} \quad (3.50)$$

where

$$\begin{aligned} \mathcal{D}(\delta\nu, \delta\lambda) &= \delta\lambda\delta\nu(\delta\lambda + \delta\nu) + ((\delta\lambda)^2 + (\delta\nu)^2)\delta\beta \\ &+ \kappa(2 - 3\kappa)(\delta\lambda + \delta\nu)(\delta\beta)^2 + 2\kappa^2(1 - 2\kappa)(\delta\beta)^3. \end{aligned} \quad (3.51)$$

This expression is $\sim 1/\delta\beta$ in agreement with (3.16) and (3.39) which are recovered when one substitutes

$$\delta\lambda = -\frac{1}{3}\delta\beta + \varepsilon\xi \quad (3.52)$$

and

$$\delta\lambda = 3\delta\beta + \varepsilon\xi, \quad (3.53)$$

respectively.

4 Critical scaling in the large- D limit

The Itzykson–Zuber integral

$$I[\phi_x, \phi_y] \equiv \int dU \, e^{Nc \operatorname{tr} \phi_x U \phi_y U^\dagger}, \quad (4.1)$$

which enters the partition functions (1.1), can easily be calculated at small c (*i.e.* at strong coupling):

$$\log I[\phi_x, \phi_y] = c \operatorname{tr} \phi_x \operatorname{tr} \phi_y + \frac{c^2 N^2}{2} \left[\frac{\operatorname{tr} \phi_x^2}{N} - \left(\frac{\operatorname{tr} \phi_x}{N} \right)^2 \right] \left[\frac{\operatorname{tr} \phi_y^2}{N} - \left(\frac{\operatorname{tr} \phi_y}{N} \right)^2 \right] + \mathcal{O}(c^3). \quad (4.2)$$

Let us consider the large- D limit of the partition function. Assuming that $V(\phi_x) \sim 1$ as $D \rightarrow \infty$,⁶ we see that the kinetic term is of order D (*i.e.* of the same order as the potential) if

$$c \sim \frac{1}{D}. \quad (4.3)$$

The Itzykson–Zuber integral coincides in this limit with the first term of the expansion (4.2) since the higher terms are suppressed. Therefore, we can write down the partition function (1.1) as

$$Z = \int \prod_x d\phi_x \, e^{-N \sum_x \operatorname{tr} V(\phi_x) + c \sum_{\{x,y\}} \operatorname{tr} \phi_x \operatorname{tr} \phi_y}. \quad (4.4)$$

Further simplification occurs in the large- N limit when we can replace one trace in the product of two traces in the exponent in (4.4) by the average value due to factorization. One arrives, hence, to the one-matrix model whose potential $\tilde{V}(\phi)$ is determined self-consistently from the equation

$$\tilde{V}(\phi) = V(\phi) - 2cD \left\langle \frac{\operatorname{tr}}{N} \phi \right\rangle_{\tilde{V}} \phi. \quad (4.5)$$

⁶We differ at this point from Ref. [4] where the large- D limit was considered for $c \sim 1$ and $V(\phi_x) \sim D$ so that the solution with the minus sign in front of the square root in Eq. (2.13) was chosen in order for μ to be ~ 1 . Contrary to the statement of Ref. [4] that there is no real scaling solutions at large D , we do have them in the limit (4.3) perturbing the Gaussian solution (2.13) with the plus sign which agrees with the large-mass expansion.

We have assumed that the potential $V(\phi)$ is not symmetric so that $\langle \text{tr } \phi \rangle \neq 0$. If $V(\phi)$ is symmetric ($V(\phi) = V(-\phi)$) and $\langle \text{tr } \phi \rangle = 0$, then one should keep the second term on the r.h.s. of Eq. (4.2) which yields

$$\tilde{V}(\phi) = V(\phi) - c^2 D \left\langle \frac{\text{tr}}{N} \phi^2 \right\rangle_{\tilde{V}} \phi^2 \quad (\text{symmetric potential}) \quad (4.6)$$

and

$$c \sim \frac{1}{\sqrt{D}} \quad (\text{symmetric potential}). \quad (4.7)$$

Eq. (4.6) is analogous to that for the one-matrix model with a symmetric potential which involves $(\text{tr } \phi^2)^2$ [10]. An equation of the type (4.5) appears [11, 12] for a non-symmetric potential. Quite similar to these papers we shall see in a moment that the KM model at large D admits scaling solutions with $\gamma_{str} \geq 0$.

Let us analyze to this aim Eq. (4.5). For the one-cut solution of the Hermitean one-matrix model with the potential \tilde{V} one gets

$$\begin{aligned} \left\langle \frac{\text{tr}}{N} \phi \right\rangle_{\tilde{V}} &= \int_{C_1} \frac{d\omega}{4\pi i} \frac{\tilde{V}'(\omega) \omega^2}{\sqrt{(\omega - x_-)(\omega - x_+)}} - \frac{x_- + x_+}{2} \\ &= \int_{C_1} \frac{d\omega}{4\pi i} \tilde{V}'(\omega) \sqrt{(\omega - x_-)(\omega - x_+)} + \frac{x_- + x_+}{2}. \end{aligned} \quad (4.8)$$

Eq. (4.5) can then be written as the following equation for \tilde{V} :

$$\tilde{V}(\lambda) = V(\lambda) - 2cD \left[\int_{C_1} \frac{d\omega}{4\pi i} \tilde{V}'(\omega) \sqrt{(\omega - x_-)(\omega - x_+)} + \frac{x_- + x_+}{2} \right] \lambda. \quad (4.9)$$

Differentiating w.r.t. a parameter of the potential which is associated with the cosmological constant and w.r.t. λ , we get finally

$$\dot{\tilde{V}}'(\lambda) = \dot{V}'(\lambda) - 2cD \int_{C_1} \frac{d\omega}{4\pi i} \dot{\tilde{V}}'(\omega) \sqrt{(\omega - x_-)(\omega - x_+)}. \quad (4.10)$$

Let us identify the cosmological constant with g_1 — the coupling in front of the linear term of the potential. For the susceptibility in genus zero one gets

$$\chi_0 = \int_{C_1} \frac{d\omega}{2\pi i} \dot{V}(\omega) \dot{E}_\omega = \dot{g}_1 \frac{(x_- - x_+)^2}{16} \quad (4.11)$$

while Eq. (4.10) yields

$$\dot{g}_1 = \frac{1}{1 + cD \frac{(x_- - x_+)^2}{8}}. \quad (4.12)$$

To obtain the critical behavior, we expand near $x_- = x_-^c$ which gives for a k -th multicritical point of the one-matrix model [23]:

$$x_- - x_-^c \sim (\tilde{g}_1^c - \tilde{g}_1)^{1/k}. \quad (4.13)$$

Under normal circumstances when Eq. (2.73) holds, one gets from (4.13)

$$\chi_0 - \chi_0^c \sim (\tilde{g}_1^c - \tilde{g}_1)^{1/k} \quad (4.14)$$

so that $\gamma_{str} = -1/k$ since

$$(g_1^c - g_1) \sim (\tilde{g}_1^c - \tilde{g}_1). \quad (4.15)$$

This is *not* the case, however, for

$$c = -\frac{8}{D(x_- - x_+)^2} \quad (4.16)$$

when the denominator in Eq. (4.12) vanishes. At this point one has

$$\dot{\tilde{g}}_1 \sim (x_- - x_-^c)^{-1} \quad (4.17)$$

so that

$$(g_1^c - g_1) \sim (\tilde{g}_1^c - \tilde{g}_1)^{(k+1)/k} \sim (x_- - x_-^c)^{k+1}. \quad (4.18)$$

For the susceptibility (2.60) one gets at the point (2.46)

$$\chi_0 \sim (x_- - x_-^c)^{-1} \sim (g_1^c - g_1)^{-1/(k+1)} \quad (4.19)$$

which is associated with $\gamma_{str} = 1/(k+1)$.

The formula (4.5), which describes the reduction of the KM model to an one-matrix model at large N in the large- D limit, can be explicitly verified for the potential (2.16) when the exact solution is known at any D . As $D \rightarrow \infty$ with $c \rightarrow 0$ according to Eq. (4.3), the potential \tilde{V} of the one-matrix model is given by the Penner potential (2.18). An explicit calculation which is based on Eq. (2.22) yields

$$\left\langle \frac{\text{tr}}{N} \phi \right\rangle_{\tilde{V}} = b - \frac{\alpha + 1}{a} \quad (4.20)$$

while the large- D limit of the potential (2.16) is

$$V(\phi) \rightarrow -\alpha \log(b - \phi) - a + 2cD \left[b - \frac{(\alpha + 1)}{a} \right] \phi \quad (4.21)$$

where (4.3) is used. It is easy to see now that Eq. (4.5) is satisfied.

While the reduction to a one-matrix model with the Penner potential holds for the KM model with the potential (2.16) in the large- D limit, the only possible scaling behavior is with $\gamma_{str} = 0$ in a perfect agreement with the results of Sect. 2. This seems to be a limiting case of $\gamma_{str} = 1/(k+1)$ which appear from the critical behavior with $\gamma_{str} = -1/k$ of the one-matrix model with the potential \tilde{V} .

Let us note finally that nonvanishing results for continuum correlators can be obtained in the large- D limit only for these of operators living at the same lattice site while the Itzykson–Zuber correlator for a contour of the length L is suppressed as

$$C(\nu, \lambda; L) \sim c^L \sim D^{-L}. \quad (4.22)$$

Therefore extended correlators vanish in the large- D limit.

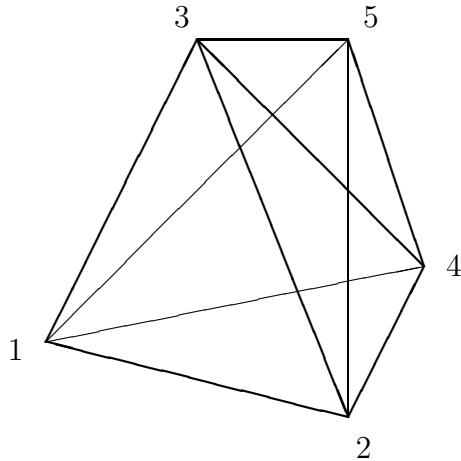


Figure 3: The lattice in the form of a q -simplex (depicted for $q = 5$).

5 The gauged Potts versus KM models

As is known, the KM model is equivalent to the matrix model on a Bethe tree [29]. We propose in this section yet another matrix model — the gauged Potts model — which is equivalent to the KM model at large N providing the coordination numbers coincide. The gauged Potts model is convenient for studying a relation with discretized random surfaces and for interpreting the results of the previous sections. The proof of equivalence is given via loop equations which reduce at large N to a one-link equation whose different forms are considered. This reduction holds in the strong coupling phase where the vacuum expectation values of the closed Wilson loops of the gauge field vanish except for those of vanishing minimal area.

5.1 The partition function

As is well-known [30], the q -state Potts model on a random lattice is equivalent to the matrix model

$$Z_{Potts} = \int \prod_{x=1}^q d\phi_x e^{N \operatorname{tr} \left(-\sum_{x=1}^q V(\phi_x) + c \sum_{x>y}^q \phi_x \phi_y \right)} \quad (5.1)$$

where the $N \times N$ Hermitean matrix ϕ_x lives on the lattice which form a q -simplex (depicted in Fig. 3 for $q = 5$). The second term in the action involves the sum over all the links (the link $\{x, y\}$ connects the sites x and y which are nothing but the vertices of the q -simplex).

We propose the following gauge-invariant extension of the model (5.1)

$$Z_{GP} = \int \prod_{x>y} dU_{xy} \prod_{x=1}^q d\phi_x e^{N \operatorname{tr} \left(-\sum_{x=1}^q V(\phi_x) + c \sum_{x>y}^q \phi_x U_{xy} \phi_y U_{xy}^\dagger \right)} \quad (5.2)$$

where the gauge variable U_{xy} lives on the link $\{x, y\}$ and dU_{xy} is the Haar measure on $U(N)$. This construction is quite similar to the KM model [2] which is described by the partition function (1.1) except the lattice is hypercubic in the latter case.

The relation of the partition function (5.1) with discretized random surfaces was studied in Ref. [30]. An analogous interpretation of the gauged Potts model (5.2) is based on the expansion (4.2) of the Itzykson–Zuber integral. Now the terms of the type $(\text{tr } \phi)^2$ generate vertices with touching surfaces [10].

5.2 Loop equations

To investigate the model (5.2), let us introduce the extended open-loop averages

$$G_{\nu\lambda}(\Gamma_{xy}) = \left\langle \frac{\text{tr}}{N} \left(\frac{1}{\nu - \phi_x} U(\Gamma_{xy}) \frac{1}{\lambda - \phi_y} U^\dagger(\Gamma_{xy}) \right) \right\rangle \quad (5.3)$$

where Γ_{xy} goes from x to y along some path on the q -simplex and the average is w.r.t. the same measure as in (5.2). $G_{\nu\lambda}(\Gamma_{xy})$ is symmetric in ν and λ due to invariance of the Haar measure dU under the transformation $U \rightarrow U^\dagger$. These quantities are quite similar to those (3.6) for the KM model.

The averages (5.3) obey quantum equations of motion which are known as the Schwinger–Dyson or loop equations. Their derivation is analogous to the one for the KM model which is presented in Appendix C and the resulting equation⁷

$$\begin{aligned} & \left\langle \frac{\text{tr}}{N} \left(\frac{V'(\phi_x)}{\nu - \phi_x} U(\Gamma_{xy}) \frac{1}{\lambda - \phi_y} U^\dagger(\Gamma_{xy}) \right) \right\rangle \\ & - \sum_{\mu=1}^{q-1} \left\langle \frac{\text{tr}}{N} \left(\phi_{x+\mu} U(\Gamma_{(x+\mu)x}) \frac{1}{\nu - \phi_x} U(\Gamma_{xy}) \frac{1}{\lambda - \phi_y} U^\dagger(\Gamma_{(x+\mu)x} \Gamma_{xy}) \right) \right\rangle \\ & = \left\langle \frac{\text{tr}}{N} \left(\frac{1}{\nu - \phi_x} \right) \frac{\text{tr}}{N} \left(\frac{1}{\nu - \phi_x} U(\Gamma_{xy}) \frac{1}{\lambda - \phi_y} U^\dagger(\Gamma_{xy}) \right) \right\rangle \\ & + \delta_{xy} \left\langle \frac{\text{tr}}{N} \left(\frac{1}{\nu - \phi_x} U(\Gamma_{xy}) \frac{1}{\lambda - \phi_y} \right) \frac{\text{tr}}{N} \left(\frac{1}{\lambda - \phi_y} U^\dagger(\Gamma_{xy}) \right) \right\rangle, \end{aligned} \quad (5.4)$$

where the sum over μ goes over

$$\Delta = q - 1 \quad (5.5)$$

directions, coincides with Eq. (C.8) providing

$$q - 1 = 2D. \quad (5.6)$$

Since Δ is nothing but the coordination number for the q -simplex which equals $2D$ for the hypercubic lattice, the equality (5.6) simply means that the coordination numbers coincide in both cases.

⁷We put $c = 1$ in this section and in Appendix C.

While the loop equations which result from the variation of ϕ_x look similar, the correlators in the second term on the r.h.s. of Eqs. (5.4) and (C.8) are, generally speaking, different. This term is proportional to δ_{xy} which does not vanish only for $x = y$, *i.e.* only for a closed contour Γ_{xx} . However, the two models are *equivalent* in the strong coupling (or small- c) phase where

$$\begin{aligned} & \left\langle \frac{\text{tr}}{N} \left(\frac{1}{\nu - \phi_x} U(\Gamma_{xx}) \frac{1}{\lambda - \phi_x} \right) \frac{\text{tr}}{N} \left(U^\dagger(\Gamma_{xx}) \frac{1}{\lambda - \phi_x} \right) \right\rangle \\ &= \delta_{0A_{\min}(\Gamma)} \frac{1}{\nu - \lambda} (E_\lambda - E_\nu) E_\lambda + \mathcal{O}\left(\frac{1}{N^2}\right) \end{aligned} \quad (5.7)$$

in both cases as $N \rightarrow \infty$. The r.h.s. of Eq. (5.7) does not vanish only for the case of contractable contours $\Gamma_{xx} = 0$ with vanishing minimal area $A_{\min}(\Gamma)$. Hence, the second term on the r.h.s. of the loop equation (5.4) vanishes for $\Gamma_{xy} \neq 0$ at $N = \infty$ independently of whether C_{xy} is closed or open.

Finally, the second term on the l.h.s. of the loop equation (5.4) can be simplified at $N = \infty$ using the formula

$$\begin{aligned} & \left\langle \frac{\text{tr}}{N} \left(\phi_{x+\mu} U(\Gamma_{(x+\mu)x}) \frac{1}{\nu - \phi_x} U(\Gamma_{xy}) \frac{1}{\lambda - \phi_y} U^\dagger(\Gamma_{(x+\mu)x} \Gamma_{xy}) \right) \right\rangle \\ &= \left\langle \frac{\text{tr}}{N} \left(\frac{F(\phi_x)}{\nu - \phi_x} U(\Gamma_{xy}) \frac{1}{\lambda - \phi_y} U^\dagger(\Gamma_{xy}) \right) \right\rangle \end{aligned} \quad (5.8)$$

which holds providing μ does not coincide with the direction of the first link of the contour Γ_{xy} emanating from the point x .

The function

$$F(\omega) = \sum_{n=0}^{\infty} F_n \omega^n, \quad F_0 = \frac{\text{tr}}{N} \left(\phi - \sum_{n=1}^{\infty} F_n \phi^n \right) \quad (5.9)$$

which enters Eq. (5.8) is determined by the pair correlator of the gauge fields

$$\frac{\int dU \, e^{\frac{\text{tr}}{N} (\phi U \psi U^\dagger)} \frac{\text{tr}}{N} (t^a U \psi U^\dagger)}{\int dU \, e^{N \text{tr} (\phi U \psi U^\dagger)}} = \sum_{n=1}^{\infty} F_n \frac{\text{tr}}{N} (t^a \phi^n) \quad (5.10)$$

where ϕ and ψ play the role of external fields and t^a ($a = 1, \dots, N^2-1$) stand for the generators of the $SU(N)$. Eq. (5.10) is based solely on the properties of the integral over unitary matrices and holds [3, 31] at $N = \infty$. The choice of F_0 which is not determined by Eq. (5.10) is a matter of convenience [7]. How to calculate the function F is explained in the next subsection.

Using (5.8) and introducing

$$\mathcal{V}'(\omega) \equiv V'(\omega) - (\Delta - 1)F(\omega), \quad (5.11)$$

we rewrite Eq. (5.4) and Eq. (C.8) at large N , when the factorization holds, in the same form

$$\int_{C_1} \frac{d\omega}{2\pi i} \frac{\mathcal{V}'(\omega)}{(\nu - \omega)} G_{\omega\lambda}(\Gamma) = E_\nu G_{\nu\lambda}(\Gamma) + \lambda G_{\nu\lambda}(\Gamma) - E_\nu + \delta_{0L(\Gamma)} \frac{1}{\nu - \lambda} (E_\lambda - E_\nu) E_\lambda \quad (5.12)$$

where the contour C_1 — the same as above — encircles counterclockwise singularities of the function $G_{\omega\lambda}(\Gamma)$.

The last term on the r.h.s. of Eq. (5.12) vanishes for $\Gamma \neq 0$ while the explicit equation for $\Gamma = 0$ reads

$$\int_{C_1} \frac{d\omega}{2\pi i} \frac{\mathcal{V}'(\omega)}{(\lambda - \omega)} E_\omega - G_1(\lambda) = E_\lambda^2 \quad (5.13)$$

where I have denoted

$$E_\lambda \equiv \left\langle \frac{\text{tr}}{N} \left(\frac{1}{\lambda - \phi_x} \right) \right\rangle \quad (5.14)$$

analogously to Eq. (2.19) for the KM model and defined the one-link average by

$$G_1(\lambda) \equiv \left\langle \frac{\text{tr}}{N} \left(\phi_{x+\mu} U(\Gamma_{(x+\mu)x}) \frac{1}{\lambda - \phi_x} U^\dagger(\Gamma_{(x+\mu)x}) \right) \right\rangle \quad (5.15)$$

since the r.h.s. does not depend on x and μ . Using Eq. (5.8) and noticing that

$$\tilde{V}'(\omega) = \mathcal{V}'(\omega) - F(\omega), \quad (5.16)$$

Eq. (5.13) can be rewritten in the form of the loop equation of the Hermitean one-matrix model

$$\int_{C_1} \frac{d\omega}{2\pi i} \frac{\tilde{V}'(\omega)}{(\lambda - \omega)} E_\omega = E_\lambda^2. \quad (5.17)$$

The explicit equation for the case when Γ coincides in Eq. (5.12) with one link reads

$$\int_{C_1} \frac{d\omega}{2\pi i} \frac{\mathcal{V}'(\omega)}{(\nu - \omega)} G_{\omega\lambda} = E_\nu G_{\nu\lambda} + \lambda G_{\nu\lambda} - E_\nu, \quad (5.18)$$

where $G_{\nu\lambda}$ is defined by Eq. (3.7). Eq. (5.13) is nothing but the $1/\lambda$ term of the expansion of Eq. (5.18) in $1/\lambda$.

Eq. (5.18) coincides with that [25] for the KM model providing the relation (5.6) holds. It can be shown that Eq. (5.12) is satisfied for any contour Γ providing Eq. (5.18) is satisfied. The open-loop averages (5.3) for the gauged Potts model coincide with those (3.6) for the KM model providing the lengths of the contours Γ_{xy} on a q -simplex and C_{xy} on a D -dimensional lattice coincide.

5.3 The general solution

Eq. (5.18) looks the same as the loop equation for the Hermitean two-matrix model [13, 14, 15]. This is because at $q = 2$, which is associated with the Hermitean two-matrix model, $\Delta = 1$ and the last term on the r.h.s. of Eq. (5.11) disappears so that one gets just $\mathcal{V}(\omega) = V(\omega)$. To analyze it, let us consider the Hermitean two-matrix model with the potential

$$\mathcal{V}(\Phi) = \sum_{m=1}^{\infty} \frac{g_m}{m} \phi^m. \quad (5.19)$$

Expanding $G_{\nu\lambda}$ in $1/\nu$

$$G_{\nu\lambda} = \frac{E_\lambda}{\nu} + \sum_{n=1}^{\infty} \frac{G_n(\lambda)}{\nu^{n+1}}, \quad G_n(\lambda) = \left\langle \frac{\text{tr}}{N} \left(\phi_x^n U_{x(x+\mu)} \frac{1}{\lambda - \phi_{x+\mu}} U_{x(x+\mu)}^\dagger \right) \right\rangle \quad (5.20)$$

and substituting into Eq. (5.18), one gets

$$\sum_{m \geq 1} g_m G_{m-1}(\lambda) = \lambda E_\lambda - 1 \quad (5.21)$$

which determines E_λ versus $\mathcal{V}(\lambda)$.

The functions $G_n(\lambda)$ are expressed via E_λ using the recurrence relation

$$G_{n+1}(\lambda) = \int_{C_1} \frac{d\omega}{2\pi i} \frac{\mathcal{V}'(\omega)}{(\lambda - \omega)} G_n(\omega) - G_0(\lambda) G_n(\lambda), \quad G_0(\lambda) = E_\lambda \quad (5.22)$$

which is obtained expanding Eq. (5.18) in $1/\lambda$. If $\mathcal{V}(\lambda)$ is a polynomial of degree J , Eq. (5.21) contains E_λ up to degree J and the solution is algebraic. As is proven in Ref. [25]:

- i) Equations which appear from the next terms of the $1/\nu$ -expansion of Eq. (5.18) are automatically satisfied as a consequence of Eqs. (5.21) and (5.22).
- ii) $G_{\nu\lambda}$ is symmetric in ν and λ for any solution of Eq. (5.21). The symmetry requirement can be used directly to determine E_λ alternatively to Eq. (5.21).

The approach based on Eq. (5.18) is equivalent [25] to that of Ref. [3] which is based on the Riemann–Hilbert method. To show this one takes the continuous and discontinuous in ν parts of $G_{\nu\lambda}$ across the cut (cuts) which are defined by Eqs. (3.9). The discontinuous part of Eq. (5.18) then reads

$$\text{Cont}_\nu G_{\nu\lambda} = 1 - \frac{1}{\text{Disc}_\nu E_\nu} \left(\lambda + \text{Cont}_\nu E_\nu - \mathcal{V}'(\nu) \right) \text{Disc}_\nu G_{\nu\lambda}, \quad \text{for } \nu \in \text{cut} \quad (5.23)$$

which coincides with the equation of Ref. [3].

To obtain a formal solution to Eq. (5.23) for $G_{\nu\lambda}$ versus E_ν , one notices that for any real ν

$$\frac{1 - G_{(\nu+i0)\lambda}}{1 - G_{(\nu-i0)\lambda}} = \frac{1 - \text{Cont}_\nu G_{\nu\lambda} - i \text{Disc}_\nu G_{\nu\lambda}}{1 - \text{Cont}_\nu G_{\nu\lambda} + i \text{Disc}_\nu G_{\nu\lambda}} = \frac{\lambda + \text{Re } E_\nu - i \text{Im } E_\nu - \mathcal{V}'(\nu)}{\lambda + \text{Re } E_\nu + i \text{Im } E_\nu - \mathcal{V}'(\nu)} \quad (5.24)$$

since $\text{Disc}_\nu G_{\nu\lambda}$ cancels at the cut (cuts) due to Eq. (5.23).

The solution to the Riemann–Hilbert problem (5.24) for $G_{\nu\lambda}$ can be expressed via E_λ as follows [3, 6, 4]

$$G_{\nu\lambda} = 1 - \exp \left\{ - \int_{C_1} \frac{d\omega}{2\pi i} \frac{1}{(\nu - \omega)} \log(\lambda - r_+(\omega)) \right\} \quad (5.25)$$

where

$$r_\pm(\lambda) = \frac{\mathcal{V}'(\lambda) + F(\lambda)}{2} \pm i\pi\rho(\lambda) = \begin{cases} \mathcal{V}'(\lambda) - E_\lambda \\ F(\lambda) + E_\lambda \end{cases}. \quad (5.26)$$

Eq. (5.25) solves Eq. (5.24) and holds for λ outside of the cut where the asymptotic expansion in $1/\lambda$ exists. It solves, hence, the recurrence relation (5.22).

5.4 Alternative one-link equations

We have obtained in the previous subsection Eq. (5.23) from Eq. (5.18). In order to show that Eq. (5.18) can be inferred, in turn, from Eq. (5.23), let us consider the following auxiliary identity

$$\begin{aligned}
\int_{C_1} \frac{d\omega}{2\pi i} \frac{\text{Cont}_\omega(E_\omega G_{\omega\lambda})}{\nu - \omega} &= E_\nu G_{\nu\lambda} - \int_{C_1} \frac{d\omega}{2\pi i} \frac{E_\omega \text{Cont}_\omega G_{\omega\lambda}}{\nu - \omega} \\
&= E_\nu G_{\nu\lambda} - E_\nu + \int_{C_1} \frac{d\omega}{2\pi i} \frac{(\lambda + \text{Cont}_\omega E_\omega - \mathcal{V}'(\omega))}{\nu - \omega} G_{\omega\lambda} = \\
E_\nu G_{\nu\lambda} - E_\nu + \lambda G_{\nu\lambda} - \int_{C_1} \frac{d\omega}{2\pi i} \frac{\mathcal{V}'(\omega)}{(\nu - \omega)} G_{\omega\lambda} + \int_{C_1} \frac{d\omega}{2\pi i} \frac{\text{Cont}_\omega(E_\omega G_{\omega\lambda})}{\nu - \omega}
\end{aligned} \tag{5.27}$$

which is based only on the analytic properties and Eq. (5.23). Canceling the l.h.s. with the last term on the r.h.s., one arrives at Eq. (5.18).

Starting from Eq. (5.23), one can derive also slightly different form of Eq. (5.18). Let us consider the inverse quantity

$$\tilde{G}_{\nu\lambda} = \frac{G_{\nu\lambda}}{1 - G_{\nu\lambda}}. \tag{5.28}$$

It is convenient to introduce

$$\mathcal{T}_{\nu\lambda} = G_{\nu\lambda} - 1 \tag{5.29}$$

and

$$\tilde{\mathcal{T}}_{\nu\lambda} = \tilde{G}_{\nu\lambda} + 1 = \frac{1}{1 - G_{\nu\lambda}} \tag{5.30}$$

so that

$$\tilde{\mathcal{T}}_{\nu\lambda} = -\mathcal{T}_{\nu\lambda}^{-1}. \tag{5.31}$$

Eq. (5.18) can be written in terms of $\mathcal{T}_{\nu\lambda}$ as

$$\int_{C_1} \frac{d\omega}{2\pi i} \frac{\mathcal{V}'(\omega)}{(\nu - \omega)} \mathcal{T}_{\omega\lambda} = E_\nu \mathcal{T}_{\nu\lambda} + \lambda \mathcal{T}_{\nu\lambda} + \lambda, \tag{5.32}$$

It follows from Eq. (5.31) that

$$\begin{aligned}
\text{Disc}_\nu \tilde{\mathcal{T}}_{\nu\lambda} &= \frac{\text{Disc}_\nu \mathcal{T}_{\nu\lambda}}{|\mathcal{T}_{\nu\lambda}|^2}, \\
\text{Cont}_\nu \tilde{\mathcal{T}}_{\nu\lambda} &= -\frac{\text{Cont}_\nu \mathcal{T}_{\nu\lambda}}{|\mathcal{T}_{\nu\lambda}|^2}
\end{aligned} \tag{5.33}$$

so that Eq. (5.23) can be rewritten as

$$\text{Cont}_\nu \tilde{\mathcal{T}}_{\nu\lambda} = \frac{1}{\text{Disc}_\nu E_\nu} \left(\lambda - \text{Cont}_\nu E_\nu - F(\nu) \right) \text{Disc}_\nu \tilde{\mathcal{T}}_{\nu\lambda}, \quad \text{for } \nu \in \text{cut}. \tag{5.34}$$

The solution to the Riemann–Hilbert problem (5.34) which is analogous to (5.25) reads

$$\tilde{\mathcal{T}}_{\nu\lambda} = \exp \left\{ - \int_{C_1} \frac{d\omega}{2\pi i} \frac{1}{(\nu - \omega)} \log(\lambda - r_-(\omega)) \right\}. \tag{5.35}$$

Moreover, these two solution coincide due to the relation (5.31).

The condition for the r.h.s. of Eq. (5.25) (or (5.35)) to be symmetric in ν and λ is given [4] by Eq. (3.14). Since $G_{\nu\lambda}$ is symmetric in ν and λ , the master field equation [3]

$$E_\lambda = \pm \int_{C_1} \frac{d\omega}{2\pi i} \log(\lambda - r_\pm(\omega)), \quad (5.36)$$

obtained as the $1/\nu$ term of Eq. (5.25), will be satisfied as a consequence of Eq. (3.14) which guarantees the symmetry.

To derive an analogue of Eq. (5.18) starting from Eq. (5.36), one proceeds similarly to (5.27):

$$\begin{aligned} \int_{C_1} \frac{d\omega}{2\pi i} \frac{\text{Cont}_\omega(E_\omega \tilde{\mathcal{T}}_{\omega\lambda})}{\nu - \omega} &= E_\nu \tilde{\mathcal{T}}_{\nu\lambda} - \int_{C_1} \frac{d\omega}{2\pi i} \frac{E_\omega \text{Cont}_\omega \tilde{\mathcal{T}}_{\omega\lambda}}{\nu - \omega} \\ &= E_\nu \tilde{\mathcal{T}}_{\nu\lambda} + \int_{C_1} \frac{d\omega}{2\pi i} \frac{(-\lambda + \text{Cont}_\omega E_\omega + F(\omega)) \tilde{\mathcal{T}}_{\omega\lambda}}{\nu - \omega} = \\ &= E_\nu \tilde{\mathcal{T}}_{\nu\lambda} - \lambda \tilde{\mathcal{T}}_{\nu\lambda} + \lambda + \int_{C_1} \frac{d\omega}{2\pi i} \frac{F(\omega)}{(\nu - \omega)} \tilde{\mathcal{T}}_{\omega\lambda} + \int_{C_1} \frac{d\omega}{2\pi i} \frac{\text{Cont}_\omega E_\omega \tilde{\mathcal{T}}_{\omega\lambda}}{\nu - \omega}. \end{aligned} \quad (5.37)$$

Hence, we get

$$\int_{C_1} \frac{d\omega}{2\pi i} \frac{F(\omega)}{(\nu - \omega)} \tilde{\mathcal{T}}_{\omega\lambda} = -E_\nu \tilde{\mathcal{T}}_{\nu\lambda} + \lambda \tilde{\mathcal{T}}_{\nu\lambda} - \lambda \quad (5.38)$$

which yields

$$\int_{C_1} \frac{d\omega}{2\pi i} \frac{F(\omega)}{(\nu - \omega)} \tilde{G}_{\omega\lambda} = -E_\nu \tilde{G}_{\nu\lambda} + \lambda \tilde{G}_{\nu\lambda} - E_\nu \quad (5.39)$$

which is an analog of Eq. (5.18) with \mathcal{V}' replaced by F . Note that with the relation (5.28) Eq. (5.39) differs from Eq. (5.18) only by the sign of the first term on the r.h.s..

Eqs. (5.21) and (5.40) are equivalent. It is a matter of practical convenience which equation to solve. Eq. (5.18) is more convenient when $\mathcal{V}'(\omega)$ is a polynomial when it reduces to an algebraic equation for E_ν . Eq. (5.39) in turn is more convenient if $F(\omega)$ is a polynomial when it reduces to an algebraic equation for E_ν .

$$\sum_{m \geq 1} F_m \tilde{G}_{m-1}(\lambda) = \lambda E_\lambda - 1 \quad (5.40)$$

and $\tilde{G}_m(\lambda)$, which are defined via the asymptotic expansion

$$\tilde{G}_{\nu\lambda} = \frac{E_\lambda}{\nu} + \sum_{n=1}^{\infty} \frac{\tilde{G}_n(\lambda)}{\nu^{n+1}}, \quad (5.41)$$

can be expressed in terms of E_λ using the recurrence relation

$$\tilde{G}_{n+1}(\lambda) = \int_{C_1} \frac{d\omega}{2\pi i} \frac{F(\omega)}{(\lambda - \omega)} \tilde{G}_n(\omega) + \tilde{G}_0(\lambda) \tilde{G}_n(\lambda), \quad \tilde{G}_0(\lambda) = E_\lambda. \quad (5.42)$$

The explicit solutions exist at any Δ for the quadratic potential [6] and the logarithmic potential (2.1) when one gets [7]

$$\mathcal{V}'(\lambda) = \frac{\alpha}{b-\lambda} - a, \quad F(\lambda) = b - \frac{\alpha+1}{a+\lambda}. \quad (5.43)$$

It is easy to verify that Eq. (5.39) is satisfied for $\tilde{G}_{\nu\lambda}$ given by (5.28) and (3.10) analogously to Eq. (5.18).

6 Discussion

The KM model with the logarithmic potential (2.1) is a very nice, explicitly solvable example of how a critical behavior can exist for $D > 1$. The analytic properties of the solution and the position of the eigenvalue support are for $\alpha < 0$ of the type advocated in Ref. [3]. From this point of view it illustrates how such unusual analytic properties can emerge in matrix models.

The continuum theories which are obtained in the vicinity of the critical lines are associated with the $\gamma_{str} = 0$ and $\gamma_{str} = -1/2$ phases of $2D$ gravity with matter independently of the fact that one starts from the matrix model on a D -dimensional lattice. Similar results can be obtained for $D = 1$ if one considers a closed matrix chain (for an open one the gauge field can be absorbed by a gauge transformation of ϕ_x). Therefore, an exact solution to this $D = 1$ problem is found for the potential (2.1).

While the phase with $\gamma_{str} = 0$ seems to coincide with the standard $d = 1$ string, a Kosterlitz–Thouless phase transition which occurs at the tri-critical point separates it from the phase with $\gamma_{str} = -1/2$ which is, however, a novel one since the continuum limit of matter at large distances sets up due to a special behavior of the Itzykson–Zuber correlator of the gauge fields. This phase never shows up, say, in the case of an open matrix chain where the gauge field can be gauged away.

The existence of these two continuum limits does not mean that a $d > 1$ phase is impossible for the KM model with the logarithmic potential on a D -dimensional lattice. An example is a two-matrix model where a nontrivial phase with $\gamma_{str} = -1/3$ realizes at a tri-critical point while generically it has $\gamma_{str} = -1/2$. It is most interesting to investigate the KM model with the potential (2.1) in the vicinity of the tri-critical point which is not done in the present paper. The point is that a singular behavior of the Itzykson–Zuber correlator, which occurs at the tri-critical point, may induce [32] a phase transition to a $d > 1$ stringy phase.

It could be, however, that the logarithmic potential (2.1) is too simple to exhibit a nontrivial scaling behavior except for $\gamma_{str} = 0$ and $\gamma_{str} = -1/2$. From this point of view the results of Sect. 4 about $\gamma_{str} > 0$ in the large- D limit for other potentials, including the quartic one, may be interesting. I do not think, however, that an exact solution can be obtained for these potentials. One should look rather for a scaling solution just near

the critical point. In particular, $1/D$ -corrections is the simplest problem to study. I hope that the fact that the mechanism of Ref. [10] of getting $\gamma_{str} > 0$ realizes for the KM model in the large- D limit can answer the question whether it corresponds to branch polymer or stringy phases.

Acknowledgements

I am indebted to J. Ambjørn, D. Boulatov, C. Kristjansen, A. Migdal, G. Semenoff, N. Weiss and K. Zarembo for very useful discussions.

Appendix A The eigenvalue support for $\alpha < 0$

To find the position of the contour C in the complex λ plane along which the spectral density, $\rho(\lambda)$, has the support for $\alpha < 0$, we apply the criterion [20] which is based for the one-cut solution (2.22) on the following integral

$$G(\lambda) = \int_{\hat{x}_-}^{\hat{\lambda}} d\tau \left[\tilde{V}'(\tau) - 2E_\tau \right]. \quad (\text{A.1})$$

The eigenvalue support is along the curve from \hat{x}_- to \hat{x}_+ determined by

$$\text{Re } G(\lambda) = 0 \quad \text{for } \lambda \in C \quad (\text{A.2})$$

which is embedded into the domain where $\text{Re } G(\lambda) < 0$. The spectral density is given by

$$\rho(\lambda) = \frac{1}{2\pi i} \frac{dG(\lambda)}{d\lambda} \quad \text{for } \lambda \in C. \quad (\text{A.3})$$

Let us consider in some detail the case $\alpha = -1$ when

$$z = \beta, \quad \hat{x}_- = \hat{x}_+ = \beta - \frac{1}{2\beta} \quad (\text{A.4})$$

according to Eqs. (2.56) and (2.37). Since the points \hat{x}_- and \hat{x}_+ coincide, C forms a closed loop which passes through the point $\beta - 1/2\beta$ and encircles the point β .

The one-cut solution (2.33) has for $\alpha = -1$ the following explicit form

$$E_\lambda = \frac{1}{2(\hat{\lambda} - \beta)} - \beta \pm \left[\frac{1}{2(\hat{\lambda} - \beta)} + \beta \right] = \begin{cases} \frac{1}{\hat{\lambda} - \beta} \\ -2\beta \end{cases} \quad (\text{A.5})$$

where the plus sign should be substituted when λ is outside of the loop C and the minus sign is associated with λ which is inside C . The expression (A.5) has the same expansion in $1/\lambda$ as an analytic continuation of the solution for positive α to $\alpha = -1$ which were give for E_λ simply $1/(\hat{\lambda} - \beta)$ with the pole at $\hat{\lambda} = \beta$. The true solution (A.5) is analytic at $\hat{\lambda} = \beta$.

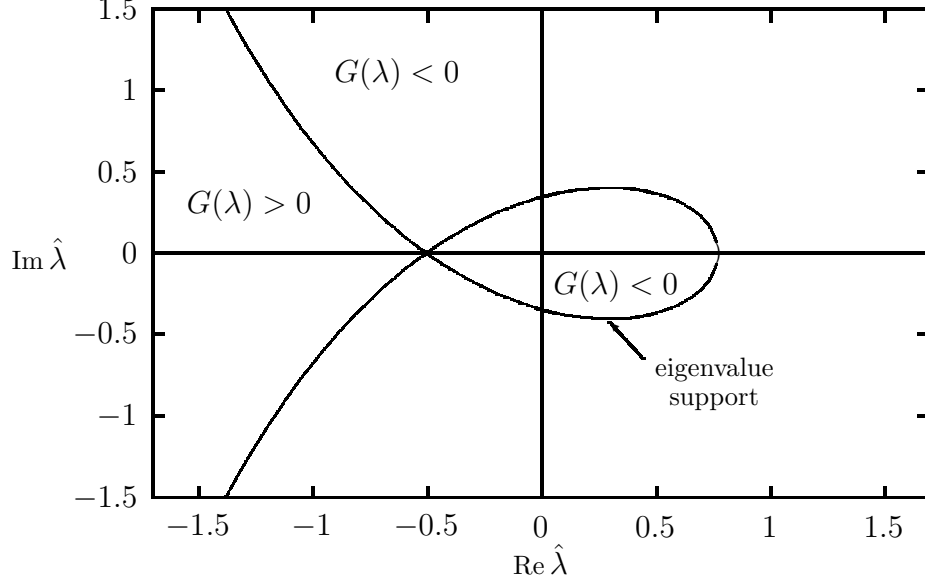


Figure 4: The eigenvalue support for $\alpha = -1$ and $\beta = 1/2$: the loop to the right of $\text{Re } \hat{\lambda} = -1/2$. The whole curve represents $G(\lambda) = 0$.

Substituting (A.5) in to Eq. (A.1) one gets

$$G(\lambda) = \pm \left[-2\beta\hat{\lambda} - \log(\hat{\lambda} - \beta) + 2\beta^2 - 1 - \log 2\beta \right]. \quad (\text{A.6})$$

Introducing the new variable κ by

$$\hat{\lambda} = \beta + \frac{1}{2\beta} \left(\kappa - \frac{1}{2} \right) \quad (\text{A.7})$$

which coincides with $\hat{\lambda}$ at $\beta = 1/2$, one rewrites Eq. (A.6) in the form

$$G(\kappa) = \mp \left[\kappa + \frac{1}{2} + \log \left(\kappa - \frac{1}{2} \right) \right] \quad (\text{A.8})$$

which does not depend explicitly on β . Denoting

$$\text{Re } \kappa = u, \quad \text{Im } \kappa = v, \quad (\text{A.9})$$

we find the solution to the equation $\text{Re } G(\kappa) = 0$ to be

$$v^2 = e^{-2u-1} - \left(u - \frac{1}{2} \right)^2. \quad (\text{A.10})$$

The curve (A.10) is depicted in Fig. 4 and is quite similar to the one for the Penner model [18]. The contour C which represents the eigenvalue support is the closed loop to the right of $u = -1/2$. The lines to the left of $u = -1/2$ separate regions of positive and negative $G(\lambda)$ which is positive to the left and negative to the right of these lines. Since $\kappa = \hat{\lambda}$ at $\beta = 1/2$, Fig. 4 represents the eigenvalue support for the $\beta = 1/2$ while that for an arbitrary $\beta > 1/2$ can be restored using Eq. (A.7).

The variables (A.9) are convenient to perform calculations with the spectral density which is determined by Eqs. (A.5) and (A.10) to be

$$\rho(\hat{\lambda}) = \frac{i\beta}{\pi} \left\{ e^{2u+1} \left(u - \frac{1}{2} - iv \right) + 1 \right\}. \quad (\text{A.11})$$

While this expression is complex, the element of probability

$$d\hat{\lambda}\rho(\hat{\lambda}) = du \frac{e^{-u-1/2} + 2u}{2\pi \sqrt{e^{-2u-1} - \left(u - \frac{1}{2}\right)^2}} \quad (\text{A.12})$$

with v given by Eq. (A.10) is real and positive. It is easy to verify the normalization condition

$$\int_{-1/2}^{u_*} du \frac{e^{-u-1/2} + 2u}{\pi \sqrt{e^{-2u-1} - \left(u - \frac{1}{2}\right)^2}} = 1 \quad (\text{A.13})$$

where $u_* = 0.77846454$ is the solution of the equation

$$e^{-u_*-1/2} - u_* + \frac{1}{2} = 0. \quad (\text{A.14})$$

Appendix B The convolution formula

We prove in this appendix that (3.22) satisfies Eq. (3.23).

Let us first change the variables $x \rightarrow 1/x$, $y \rightarrow 1/y$ and rewrite Eq. (3.22) as

$$C_c\left(\frac{1}{x}, \frac{1}{y}; \sqrt{u}\right) = x^2 y^2 \hat{C}(x, y; \sqrt{u}) \quad (\text{B.1})$$

with

$$\hat{C}(x, y; \sqrt{u}) = \frac{2\sqrt{u}}{(x-y)^2 + 2u(x+y) + u^2}. \quad (\text{B.2})$$

Substituting $t \rightarrow 1/t$, we rewrite Eq. (3.23) as

$$\frac{1}{\pi} \int_0^\infty dt \sqrt{t} \hat{C}(x, t; \sqrt{u}) \hat{C}(t, y; \sqrt{v}) = \hat{C}(x, y; \sqrt{u} + \sqrt{v}). \quad (\text{B.3})$$

To prove Eq. (B.3), let us calculate the integral on the l.h.s. taking residues at $t = t_\pm(x)$ and $t = t_\pm(y)$ with

$$t_\pm(x) = x - u \pm 2i\sqrt{xu} \quad (\text{B.4})$$

and

$$t_\pm(y) = y - v \pm 2i\sqrt{yv} \quad (\text{B.5})$$

being the poles of $\hat{C}(x, t; \sqrt{u})$ or $\hat{C}(t, y; \sqrt{v})$, respectively. Since $t_+(x)$ and $t_-(x)$ (or $t_+(y)$ and $t_-(y)$) lie on the opposite sides of the branch cut of \sqrt{t} which goes along positive real axis as in depicted in Fig. 5, we get

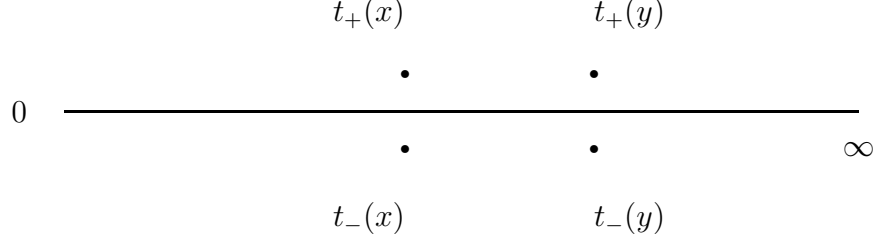


Figure 5: The position of the cut of $\rho_c(t)$ in the t -plane (the bold line) and the positions of the poles of the integrand in Eq. (B.9), $t_{\pm}(x)$ and $t_{\pm}(y)$, which are given by Eqs. (B.4) and (B.5), respectively.

$$\sqrt{t_+(x)} = \sqrt{x} + i\sqrt{u}, \quad \sqrt{t_-(x)} = -\sqrt{x} + i\sqrt{u} \quad (\text{B.6})$$

and

$$\sqrt{t_+(y)} = \sqrt{y} + i\sqrt{v}, \quad \sqrt{t_-(y)} = -\sqrt{y} + i\sqrt{v}. \quad (\text{B.7})$$

Collecting the contribution from all four poles, factoring the common denominator as

$$\begin{aligned} & [(x-y)^2 + 2(x+y)(u+v) + (u-v)^2]^2 - 64xyuv \\ &= [(x-y)^2 + 2(\sqrt{u} + \sqrt{v})^2(x+y) + (\sqrt{u} + \sqrt{v})^4] \\ & \cdot [(x-y)^2 + 2(\sqrt{u} - \sqrt{v})^2(x+y) + (\sqrt{u} - \sqrt{v})^4] \end{aligned} \quad (\text{B.8})$$

and cancelling the last factor with the numerator, we get finally

$$\begin{aligned} & \frac{1}{\pi} \int_0^\infty \frac{dt\sqrt{t}}{[(x-t)^2 + 2u(x+t) + u^2][(y-t)^2 + 2v(y+t) + v^2]} \\ &= \frac{\sqrt{u} + \sqrt{v}}{2\sqrt{uv}} \frac{1}{[(x-y)^2 + 2(\sqrt{u} + \sqrt{v})^2(x+y) + (\sqrt{u} + \sqrt{v})^4]}. \end{aligned} \quad (\text{B.9})$$

This completes the proof of Eq. (B.3).

Appendix C Derivation of the loop equations

Loop equations of the KM model or the gauged Potts model result, as usual, from the invariance of the integration measure under an infinitesimal shift of fields. One distinguishes equations resulting from the shift of the matter fields ϕ_x (that gives, in particular, the lattice Klein–Gordon equation) and that of the gauge field U_{xy} (that gives, in particular, the lattice Maxwell equation in the case of the standard lattice gauge theory).

C.1 Matter loop equation

Let us consider an equation which results from the invariance of the measure over ϕ in the open-loop average (3.6) under an infinitesimal shift

$$\phi_x \rightarrow \phi_x + \xi_x \quad (\text{C.1})$$

of ϕ_x at the given site x with ξ_x being an infinitesimal Hermitean matrix. For ϕ_x being a matrix from the adjoint representation of $SU(N)$, one should impose $\text{tr } \xi_x = 0$ in order for the shifted matrix to belong to the adjoint representation as well. For the general Hermitean matrices ϕ_x , ξ_x is arbitrary Hermitean.

These two cases can be considered simultaneously introducing N^2 generators

$$[t^A]_{ij} = \left(\delta_{ij}, [t^a]_{ij} \right) \quad (\text{C.2})$$

with t^a ($a = 1, \dots, N^2-1$) being the standard generators of $SU(N)$. The generators (C.2) obey the following normalization

$$\frac{\text{tr}}{N} t^A t^B = \delta^{AB} \quad (\text{C.3})$$

and completeness condition

$$[t^A]_{ij} [t^A]_{kl} = N \delta_{il} \delta_{kj}. \quad (\text{C.4})$$

An arbitrary $N \times N$ Hermitean matrix ϕ can be represented as

$$\phi = t^A \phi^A \quad \text{where} \quad \phi^A = \left(\frac{\text{tr}}{N} \phi, \frac{\text{tr}}{N} t^a \phi \right) \quad (\text{C.5})$$

with $\phi^0 = \frac{\text{tr}}{N} \phi$ vanishing if ϕ is taken in the adjoint representation of $SU(N)$.

To derive the loop equation I apply a trick similar to that used in deriving loop equations of QCD [17]. Let us consider the loop average

$$\left\langle \frac{\text{tr}}{N} \left(t^A \frac{1}{\nu - \phi_x} U(C_{xy}) \frac{1}{\lambda - \phi_y} U^\dagger(C_{xy}) \right) \right\rangle = 0, \quad (\text{C.6})$$

where the averaging is taken with the same measure as in Eq. (1.1), which vanishes due to the gauge invariance. Performing the shift (C.1) of ϕ_x , using the invariance of the measure and calculating $\partial/\partial\phi_x^B$, one gets

$$\begin{aligned} & \left\langle \frac{\text{tr}}{N} \left(t^B V'(\phi_x) \right) \frac{\text{tr}}{N} \left(t^A \frac{1}{\nu - \phi_x} U(C_{xy}) \frac{1}{\lambda - \phi_y} U^\dagger(C_{xy}) \right) \right\rangle \\ & - \sum_{\substack{\mu=-D \\ \mu \neq 0}}^D \left\langle \frac{\text{tr}}{N} \left(t^B U_{x(x+\mu)} \phi_{x+\mu} U_{x(x+\mu)}^\dagger \right) \frac{\text{tr}}{N} \left(t^A \frac{1}{\nu - \phi_x} U(C_{xy}) \frac{1}{\lambda - \phi_y} U^\dagger(C_{xy}) \right) \right\rangle \\ & = \left\langle \frac{\text{tr}}{N^3} \left(t^A \frac{1}{\nu - \phi_x} t^B \frac{1}{\nu - \phi_x} U(C_{xy}) \frac{1}{\lambda - \phi_y} U^\dagger(C_{xy}) \right) \right\rangle \\ & + \delta_{xy} \left\langle \frac{\text{tr}}{N^3} \left(t^A \frac{1}{\nu - \phi_x} U(C_{xy}) \frac{1}{\lambda - \phi_y} t^B \frac{1}{\lambda - \phi_y} U^\dagger(C_{xy}) \right) \right\rangle. \quad (\text{C.7}) \end{aligned}$$

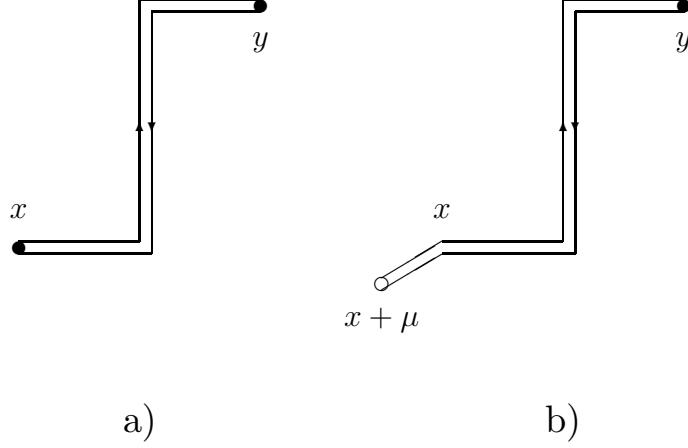


Figure 6: The graphic representation for $G_{\nu\lambda}(C_{xy})$ (a) and $G_{\nu\lambda}(C_{(x+\mu)x}C_{xy})$ (b) entering Eq. (5.12). The empty circle represents $\phi_{x+\mu}$ while the filled ones represent $\frac{1}{\nu-\phi_x}$ or $\frac{1}{\lambda-\phi_y}$. The oriented solid lines represent the path-ordered products $U(C_{xy})$ and $U(C_{(x+\mu)x}C_{xy})$. The color indices are contracted according to the arrows.

The l.h.s. of this equation results from the variation of the action while the r.h.s. represents the commutator term resulting from the variation of the integrand.

The averaging over the gauge group picks up two nonvanishing invariant equations for the Hermitean matrices. The first one can be obtained contracting Eq. (C.7) by δ^{AB} ($A, B = 0, \dots, N^2-1$) while the second one is given by the $A, B = 0$ component.

The first equation for the Hermitean model reads

$$\begin{aligned}
& \left\langle \frac{\text{tr}}{N} \left(\frac{V'(\phi_x)}{\nu - \phi_x} U(C_{xy}) \frac{1}{\lambda - \phi_y} U^\dagger(C_{xy}) \right) \right\rangle \\
& - \sum_{\substack{\mu=-D \\ \mu \neq 0}}^D \left\langle \frac{\text{tr}}{N} \left(\phi_{x+\mu} U(C_{(x+\mu)x}) \frac{1}{\nu - \phi_x} U(C_{xy}) \frac{1}{\lambda - \phi_y} U^\dagger(C_{(x+\mu)x}C_{xy}) \right) \right\rangle \\
& = \left\langle \frac{\text{tr}}{N} \left(\frac{1}{\nu - \phi_x} \right) \frac{\text{tr}}{N} \left(\frac{1}{\nu - \phi_x} U(C_{xy}) \frac{1}{\lambda - \phi_y} U^\dagger(C_{xy}) \right) \right\rangle \\
& + \delta_{xy} \left\langle \frac{\text{tr}}{N} \left(\frac{1}{\nu - \phi_x} U(C_{xy}) \frac{1}{\lambda - \phi_y} \right) \frac{\text{tr}}{N} \left(\frac{1}{\lambda - \phi_y} U^\dagger(C_{xy}) \right) \right\rangle \quad (C.8)
\end{aligned}$$

where the path $C_{(x+\mu)x}C_{xy}$ on the l.h.s. is obtained by attaching the link $(x, x + \mu)$ to the path C_{xy} at the end point x as is depicted in Fig. 6. Using the definition (3.6), this equation can be written finally at large N in the form (5.12).

The second equation which is given by the $A, B = 0$ component of Eq. (C.7) reads

$$\begin{aligned}
& \left\langle \left(\frac{\text{tr}}{N} V'(\phi_x) - \sum_{\substack{\mu=-D \\ \mu \neq 0}}^D \frac{\text{tr}}{N} \phi_{x+\mu} \right) \frac{\text{tr}}{N} \frac{1}{\nu - \phi_x} U(C_{xy}) \frac{1}{\lambda - \phi_y} U^\dagger(C_{xy}) \right\rangle \\
&= \left\langle \frac{\text{tr}}{N^3} \frac{1}{(\nu - \phi_x)^2} U(C_{xy}) \frac{1}{(\lambda - \phi_y)} U^\dagger(C_{xy}) \right\rangle \\
&+ \delta_{xy} \left\langle \frac{\text{tr}}{N^3} \frac{1}{(\nu - \phi_x)} U(C_{xy}) \frac{1}{(\lambda - \phi_y)^2} U^\dagger(C_{xy}) \right\rangle.
\end{aligned} \tag{C.9}$$

In the large- N limit when the factorization holds, Eq. (C.9) is automatically satisfied as a consequence of the $\mathcal{O}((\nu\lambda)^{-1})$ term in Eq. (C.8).

When the matrices ϕ_x belong to the *adjoint* representation of $SU(N)$, there exists only one invariant which results from contracting Eq. (C.7) by δ^{ab} ($a, b = 1, \dots, N^2-1$). The point is that the $B = 0$ component does not appear since solely the variation $\partial/\partial\phi_x^b$ is permitted for the adjoint-representation matrices. Therefore, in order to obtain an analog of Eq. (C.8) for the adjoint scalars, one should subtract the l.h.s. of Eq. (C.9) from its l.h.s. and the r.h.s. of Eq. (C.9) from the r.h.s. to kill the $A=B=0$ component. The result differs from Eq. (C.8) by contact terms which enter Eq. (C.9) and should not survive as $N \rightarrow \infty$. The vanishing of these contact terms in the large- N limit, when the factorization holds, is obvious for an even potential $V(\phi) = V(-\phi)$.

C.2 Maxwell open-loop equation

The open-loop averages (3.6) obey one more loop equation which results from the invariance of the Haar measure over $U_{x(x+\mu)}$ under the shift

$$U_{x(x+\mu)} \rightarrow (1 + i\epsilon_{x(x+\mu)})U_{x(x+\mu)} \tag{C.10}$$

of $U_{x(x+\mu)}$ at the link (x, μ) with $\epsilon_{x(x+\mu)}$ being an infinitesimal traceless Hermitean matrix.

The loop equation can again be obtained by the trick [17]. Let us consider the loop average

$$\left\langle \frac{\text{tr}}{N} \left(\frac{1}{\nu - \phi_x} U(C_{xz}) t^A U^\dagger(C_{xz}) \right) \frac{\text{tr}}{N} \left(t^B U(C_{zy}) \frac{1}{\lambda - \phi_y} U^\dagger(C_{zy}) \right) \right\rangle = 0, \tag{C.11}$$

where the averaging is taken with the same measure as in Eq. (1.1), which vanishes due to the gauge invariance. Performing the shift (C.10) of $U_{z(z+\mu)}$ at some link $(z, \mu) \in C_{xy}$

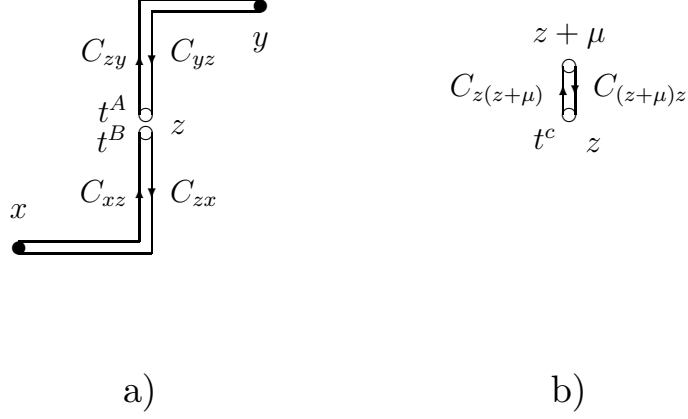


Figure 7: The contours C_{xz} (C_{zx}) or C_{zy} (C_{yz}) (a) and $C_{(x+\mu)x}$ ($C_{x(x+\mu)}$) (b) for Eq. (C.12).

and using the invariance of the Haar measure, one gets

$$\begin{aligned}
& \left\langle \frac{\text{tr}}{N} \left(\frac{1}{\nu - \phi_x} U(C_{xz}) t^A U^\dagger(C_{xz}) \right) \frac{\text{tr}}{N} \left([t^B, t^c] U(C_{zy}) \frac{1}{\lambda - \phi_y} U^\dagger(C_{zy}) \right) \right. \\
& + \frac{\text{tr}}{N} \left(\frac{1}{\nu - \phi_x} U(C_{xz}) t^A U^\dagger(C_{xz}) \right) \frac{\text{tr}}{N} \left(t^B U(C_{zy}) \frac{1}{\lambda - \phi_y} U^\dagger(C_{zy}) \right) \\
& \left. \cdot N \frac{\text{tr}}{N} \left([\phi_z, t^c] U_\mu(z) \phi_{z+\mu} U_\mu^\dagger(z) \right) \right\rangle = 0 \quad (\text{C.12})
\end{aligned}$$

where the contours are depicted in Fig. 7.

The desired loop equation can be obtained contracting Eq. (C.12) by the structure constant f^{abc} which is defined by the commutator

$$[t^a, t^b] = i f^{abc} t^c. \quad (\text{C.13})$$

The normalizations are fixed by Eq. (C.3) which gives

$$f^{abc} f^{dbc} = 2N \delta^{ab}. \quad (\text{C.14})$$

I shall utilize as well the following formulas

$$i f^{abc} [t^a]_{ij} [t^b]_{kl} = [t^c]_{il} \delta_{kj} - [t^c]_{kj} \delta_{il} \quad (\text{C.15})$$

and

$$i f^{abc} [t^a]_{ij} [t^b]_{kl} [t^c]_{mn} = N (\delta_{il} \delta_{kn} \delta_{mj} - \delta_{in} \delta_{kj} \delta_{ml}). \quad (\text{C.16})$$

Eq. (C.16) can be obtained from Eq. (C.15) multiplying by $[t^c]_{mn}$ and substituting the completeness condition Eq. (C.4). Eq. (C.16) was used, in particular, in studies [33] of loop equations of QCD.

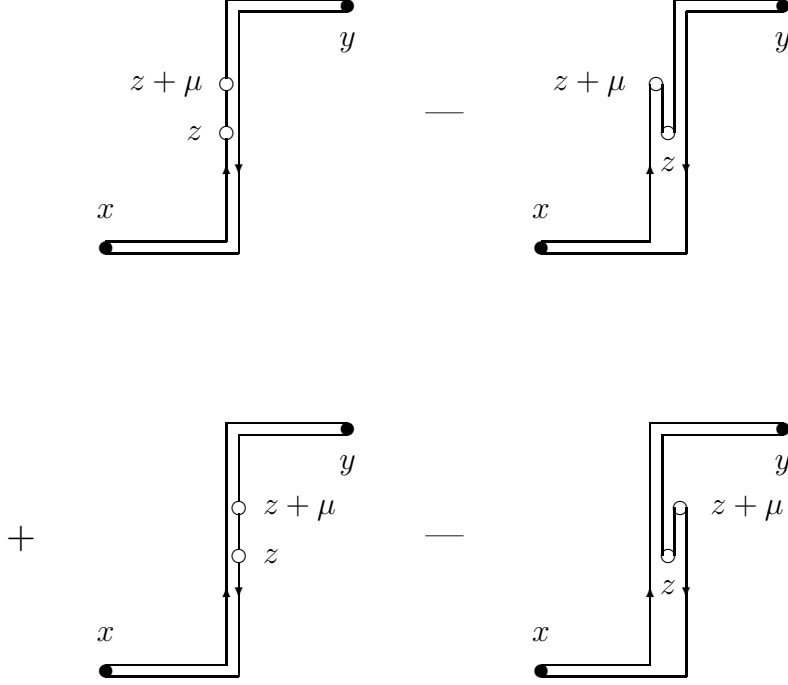


Figure 8: The graphic representation of the r.h.s. of Eq. (C.17).

The result of contracting Eq. (C.12) by if^{abc} reads

$$\begin{aligned}
& \left\langle \frac{\text{tr}}{\text{N}} \left(\frac{1}{\nu - \phi_x} U(C_{xy}) \frac{1}{\lambda - \phi_y} U^\dagger(C_{zy}) \right) - \frac{\text{tr}}{\text{N}} \frac{1}{\nu - \phi_x} \frac{\text{tr}}{\text{N}} \frac{1}{\lambda - \phi_y} \right\rangle \\
&= \frac{1}{2} \left\langle \frac{\text{tr}}{\text{N}} \left(\frac{1}{\nu - \phi_x} \left[U(C_{xz}) \phi_z U(C_{z(z+\mu)}) \phi_{z+\mu} U(C_{(z+\mu)y}) \frac{1}{\lambda - \phi_y} U^\dagger(C_{xy}) \right. \right. \right. \\
&\quad \left. \left. \left. - U(C_{x(z+\mu)}) \phi_{z+\mu} U^\dagger(C_{z(z+\mu)}) \phi_z U(C_{zy}) \frac{1}{\lambda - \phi_y} U^\dagger(C_{xy}) \right. \right. \right. \\
&\quad \left. \left. \left. + U(C_{xy}) \frac{1}{\lambda - \phi_y} U^\dagger(C_{(z+\mu)y}) \phi_{z+\mu} U^\dagger(C_{z(z+\mu)}) \phi_z U^\dagger(C_{x(z+\mu)}) \right. \right. \right. \\
&\quad \left. \left. \left. - U(C_{xy}) \frac{1}{\lambda - \phi_y} U^\dagger(C_{zy}) \phi_z U(C_{z(z+\mu)}) \phi_{z+\mu} U^\dagger(C_{x(z+\mu)}) \right] \right) \right\rangle. \quad (\text{C.17})
\end{aligned}$$

where the contours entering the r.h.s. are depicted in Fig. 8.

Note that quantities of a new type appears on the r.h.s. of Eq. (C.17) so that the set of equations is not closed. The meaning of this equation is that it expresses the one-link correlator of $UUU^\dagger U^\dagger$ via the correlator of UU^\dagger , *i.e.* via $C(x, y)$.

References

- [1] J. Ambjørn, *Barriers in quantum gravity*, preprint NBI-HE-93-31 (July, 1993).
- [2] V.A. Kazakov and A.A. Migdal, *Nucl. Phys.* **B397** (1993) 214.
- [3] A.A. Migdal, *Mod. Phys. Lett.* **A8** (1993) 359; **A8** (1993) 153.
- [4] D.V. Boulatov, *Critical scaling in the matrix model on a Bethe tree*, preprint NBI-HE-93-55 (September, 1993), hep-th/9309100.
- [5] A. Matytsin and A.A. Migdal, *Edge singularity in “induced QCD”*, preprint PUPT-1460 (April, 1994), hep-th/9404096.
- [6] D. Gross, *Phys. Lett.* **293B** (1992) 181.
- [7] Yu. Makeenko, *Phys. Lett.* **314B** (1993) 197.
- [8] Yu. Makeenko, *Matrix models of induced QCD*, in Proc. of the XXVII International Ahrenshoop symposium on the Theory of Elementary Particles, eds. D. Lüst and G. Weigt, DESY 94-053 (March 1994), pp. 85–100.
- [9] L. Paniak and N. Weiss, unpublished.
- [10] S.R. Das, A. Dhar, A.M. Sengupta and S.R. Wadia, *Mod. Phys. Lett.* **A5** (1990) 1041.
- [11] G.P. Korchemsky, *Mod. Phys. Lett.* **A7** (1992) 3081.
- [12] L. Alvarez-Gaumé, J.L. Barbón and Č. Crnković, *Nucl. Phys.* **B394** (1993) 393.
- [13] E. Gava and K.S. Narain, *Phys. Lett.* **263B** (1991) 213.
- [14] J. Alfaro, *Phys. Rev.* **D47** (1993) 4714.
- [15] M. Staudacher, *Phys. Lett.* **305B** (1993) 332.
- [16] R.C. Penner, *Comm. Math. Phys.* **113** (1987) 299; *J. Diff. Geom.* **27** (1988) 35.
- [17] A.A. Migdal, *Phys. Rep.* **102** (1983) 199.
- [18] S. Chaudhuri, H. Dykstra and J. Lykken, *Mod. Phys. Lett.* **A6** (1991) 1665.
- [19] J. Ambjørn, C.F. Kristjansen and Yu. Makeenko, *Generalized Penner models beyond the spherical limit*, preprint NBI-HE-94-14, (January, 1994), hep-th/9403024.
- [20] F. David, *Nucl. Phys.* **B348** (1991) 507.
- [21] E. Brézin, C. Itzykson, G. Parisi and J.B. Zuber, *Commun. Math. Phys.* **59** (1978) 35.
- [22] C.-I Tan, *Mod. Phys. Lett.* **A6** (1991) 1373; *Phys. Rev.* **D45** (1992) 2862.
- [23] V.A. Kazakov, *Mod. Phys. Lett.* **A4** (1989) 2125.
- [24] Yu. Makeenko, *Mod. Phys. Lett.* **A8** (1993) 209.
- [25] M.I. Dobroliubov, Yu. Makeenko and G.W. Semenoff, *Mod. Phys. Lett.* **A8** (1993) 2387.
- [26] M.I. Dobroliubov, A. Morozov, G.W. Semenoff and N. Weiss, *Evaluation of observables in the Gaussian $N = \infty$ Kazakov–Migdal model*, preprint UBC-27/93, (December, 1993), hep-th/9312145.
- [27] D.J. Gross and I.R. Klebanov, *Nucl. Phys.* **B344** (1990) 475.
- [28] Z. Yang, *Phys. Lett.* **243B** (1990) 365.

- [29] D. Boulatov, *Mod. Phys. Lett.* **A8** (1993) 557.
- [30] V.A. Kazakov, *Nucl. Phys. B* (Proc. Suppl.) **4** (1988) 93.
- [31] A.A. Migdal, *Mod. Phys. Lett.* **A8** (1993) 245.
- [32] M.I. Dobroliubov, I.I. Kogan, G.W. Semenoff and N. Weiss, *Phys. Lett.* **302B** (1993) 283.
- [33] Yu.M. Makeenko and A.A. Migdal, *Nucl. Phys.* **B188** (1981) 269.